NASA CR-54303

DEVELOPMENT OF HIGH TEMPERATURE CERAMIC RECTIFIERS, THYRATRONS, AND VOLTAGE REGULATOR TUBES

by

E. A. Baum

prepared for

NATIONAL AERONAUTICS AND SPACE ADMINISTRATION

CONTRACT NAS3-2548

GENERAL ELECTRIC

Development of

HIGH TEMPERATURE CERAMIC RECTIFIERS, THYRATRONS, AND VOLTAGE REGULATOR TUBES

Final Report
June 26, 1963 through October 7, 1964

Contract No. NAS3-2548

Technical Management
NASA-Lewis Research Center
Solar and Chemical Power Branch
Ernest A. Koutnik

E. A. Baum
Schenectady Tube Operation
Tube Department
General Electric Company
Schenectady, New York 12305

References:

Control No. SEPO-1038
G-E File No. SD-514
October 25, 1963

TABLE OF CONTENTS

LIST OF ILLUSTRATIONS

FINAL REPORT CONTRACT NAS3-2548

FOREWORD

The report has been prepared by the Schenectady Tube Operation, General Electric Company under National Aeronautics and Space Administration Contract NAS3-2548.

This work was administered under the direction of Mr. E. A. Koutnik of the Space Power Systems Division, Lewis Research Center, Cleveland, Ohio.

This report covers the work performed from 26 June 1963 to 7 October 1964 by the General Electric Tube Department, Schenectady Tube Operation.

SUMMARY

The work effort on this program was directed toward the determination of any major limitations in the operation of voltage regulator tubes, gas diodes, and thyratrons to temperatures up to 800°C. Since the problems involved in the development of the vacuum envelope for such tubes is the same, a single ceramic-to-metal seal evaluation was made. Two types of seals were evaluated up to 850°C in vacuum:

1) active alloy enriched nickel-titanium seals
2) the metallized type seal

The results showed that both types of seals could operate at this temperature for periods beyond 2000 hours. Some seals tested accumulated over 3500 hours without failure.

Two cathode systems were considered for the rectifier and thyratron tubes:

1) the barium system
2) the thoriated cathode system

Since the barium system has the advantage in efficiency, it was chosen for evaluations. Evaporation rate measurements were made on the barium orthosilicate dispenser cathode and on a high emission density tungstate cathode. The results indicate that the evaporation rate associated with the required operating temperature for high emission densities would be prohibitive for long term operation.

Investigations of the back emission were made on possible anode and grid materials. The results showed that pyrolitic impregnated graphite would have minimum emission under actual tube conditions. Based on these results a high temperature ceramic test diode was designed, fabricated, and operated at 800°C ambient temperature. The diodes were xenon filled and were run over the frequency range of 60 cps to 3200 cps, with peak inverse voltages up to 1000 volts. While no direct measurements were made of the gas clean-up rate, observations indicated that this was not excessive. Extended operating times are required before an evaluation of this type can be made.

Ceramic voltage regulator tubes were operated up to 800°C in vacuum. The gas was neon at a pressure of 60 Torr at 800°C. Regulation was found to be within 2 to 3 percent over a 25 to 75 milliampere current range. The effects of step changes in current were also observed for neon pressures of 45 to 80 Torr and a tube temperature 800°C. Maximum voltage variations of 0.5 volt were found for 10-milliampere step changes in current with stabilization times of 5 to 10 minutes.

INTRODUCTION

This final report on Contract NAS3-2548 covers the period 26 June to 7 October 1964. The work effort on this program was directed toward the development of high-temperature, high-power-level gas tubes. The objective of the over-all program is the development of high-temperature ceramic rectifiers, thyratrons, and voltage regulator tubes for long term use in nuclear electric space power systems. This phase of the effort was for the purpose of investigating fundamental problems that limit the operation of high-temperature, high-frequency gas tubes. During this phase an investigation was made to establish solutions to problems limiting device capability. The four general tasks were as follows:

Task 1

Extend ratings of high-temperature rectifiers and thyratrons to 0.150, 2.0, and 10 ampere capacity, 750 volt PIV, up to 3200 c/s, capable of operation at 800°C.

Task 2

Investigate voltage regulator tubes capable of operation at 800°C in vacuum.

Task 3

Investigate problems associated with the development of high-power, high-temperature ceramic rectifiers.

Task 4

Investigate problems associated with the development of high-power, high-temperature ceramic thyratrons.

The extension of operating temperatures of gaseous discharge devices beyond 500°C requires state-of-the-art advances in materials technology and design concepts. The major problem areas in such a development are:

1) ceramic-to-metal seals capable of long life in the temperature range of 600° to 900°C

2) gas clean-up rates under high-temperature, high-frequency conditions

3) anode work function variations resulting in back emission

4) thermal requirements encountered in designing the tube component to fit a given system

During this contract period, these four problem areas were investigated. These investigations were limited, both in time and scope, as necessitated by the work effort, to the determination of any major limitations. Ceramic tubes of the rectifier and voltage-regulator type were operated under the given conditions of temperature and frequency. As a result of this effort, conceptual designs of ceramic tubes have been produced and will be evaluated further on any subsequent effort.

TECHNICAL DISCUSSION AND PROGRESS

CERAMIC SEALS

Materials

The problems involved in the development of a vacuum envelope for high ceramic diodes, thyratrons, and voltage regulator tubes under similar operating conditions are essentially the same and therefore a single investigation was made in the ceramic seal area. Two types of seals were investigated during this contract:

1) active alloy seals utilizing enriched nickel-titanium seals

2) metallized ceramic seals

In the first type of seal the braze material is active; that is, it can wet and form a bond to the ceramic when molten. The metallized ceramic technique, however, requires that a coating of refractory metal be bonded to the surface to provide a metallic surface to which conventional braze materials can adhere. Generally, the metallized coating consists of a refractory metal such as molybdenum mixed with a metal oxide and sintered to the ceramic surface. Conventional braze materials can then be used.

The seal evaluation work effort under this contract was limited to extended tests at approximately 850°C in vacuum for both types of seals.

Test Procedure

A high-temperature vacuum test system was constructed for the seal evaluation. The system utilized two ceramic vacuum chambers which were inserted into temperature controlled ovens capable of attaining temperatures of approximately 1025°C. The test seals were placed on a molybdenum or tantalum boat and then placed into the ceramic vessel. Three circular disc baffles were inserted near the exhaust end of the ceramic cylinders to prevent heat loss by radiation down the cylinder. The ceramic cylinder was sealed to the vacuum system by means of an O-ring flange. The two chambers were continually pumped through a common exhaust chamber as shown in Figure 1. Valves in the high-vacuum line allowed either chamber to be closed off from the vacuum

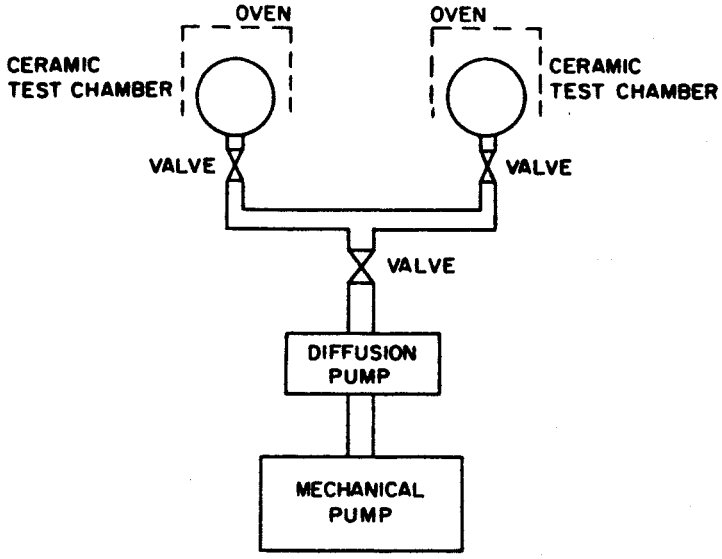

Figure 1 - Schematic Diagram of Test System for Life Testing Seals

system and opened to air while the other chamber remained under vacuum. Figure 2 shows the completed system in operation. The cubicle at the right contains the diffusion and mechanical pumps. The mechanical roughing pump is mounted below the table along with a 5 KVA voltage regulator. Temperature controls are seen on the back wall above the furnaces, and the vacuum-test chamber is the ceramic tube mounted on the exhaust manifold. The ceramic cylinder is inserted in the hole in the oven door.

During test procedures the pump was evacuated to approximately 2×10^{-5} Torr. The ovens were then turned on and brought slowly up to temperature. System pressure during this period was maintained at between 2 and 5×10^{-5} Torr. Temperature was maintained by a thermocouple inserted along the outside of ceramic cylinder to about the midpoint of the oven. Every 200 to 500 hours the samples were removed from the test chamber, leak checked, and then reinserted and continued on test.

Figure 3 shows a schematic of the test samples. The active alloy test seals were of the butt seal type. The body ceramic and the back-up ceramics were 97% alumina (A923). Nickel seal flanges .010 inch thick were used and the seals were affected by using a titanium shim .0005 inch thick. Seven seals of this type were made at brazing temperatures ranging between 1260°C and 1320°C. Of these seven samples, seal No. 2 failed during the first 200 hours. This seal was brazed at 1260°C. Samples 3 and 4 accumulated 2150 hours, and seal 5 accumulated 2175 hours. At the time they were removed from test, seals 4 and 5 were still vacuum tight. During this run the oven temperature increased to 1000°C because of a malfunction of the oven control. Sample 1 accumulated 3730 hours before being removed from the test chamber, and seals 6 and 7 accumulated 3750 hours.

Initially, test samples of the metallized seals were made to determine the best firing schedule for the molybdenum-manganese metallized coating. Tests were made on the 97% alumina body and the 94% alumina body using a metallizing composition of 70-30 wgt-% Mo-Mn. Six test samples of each ceramic body were prepared. Three samples of each body type were metallized at 1480°C and three each at 1560°C. The seals were brazed at 1050°C with a 65-35 wgt-% copper-gold braze material. Of the six samples metallized at 1480°C on 97% alumina, one leaked and the rest were tight, but the seals appeared questionable. The bonding mechanism of the metallized coating depends on the interaction of the manganese and the alumina. At temperatures in the region of 1450 to

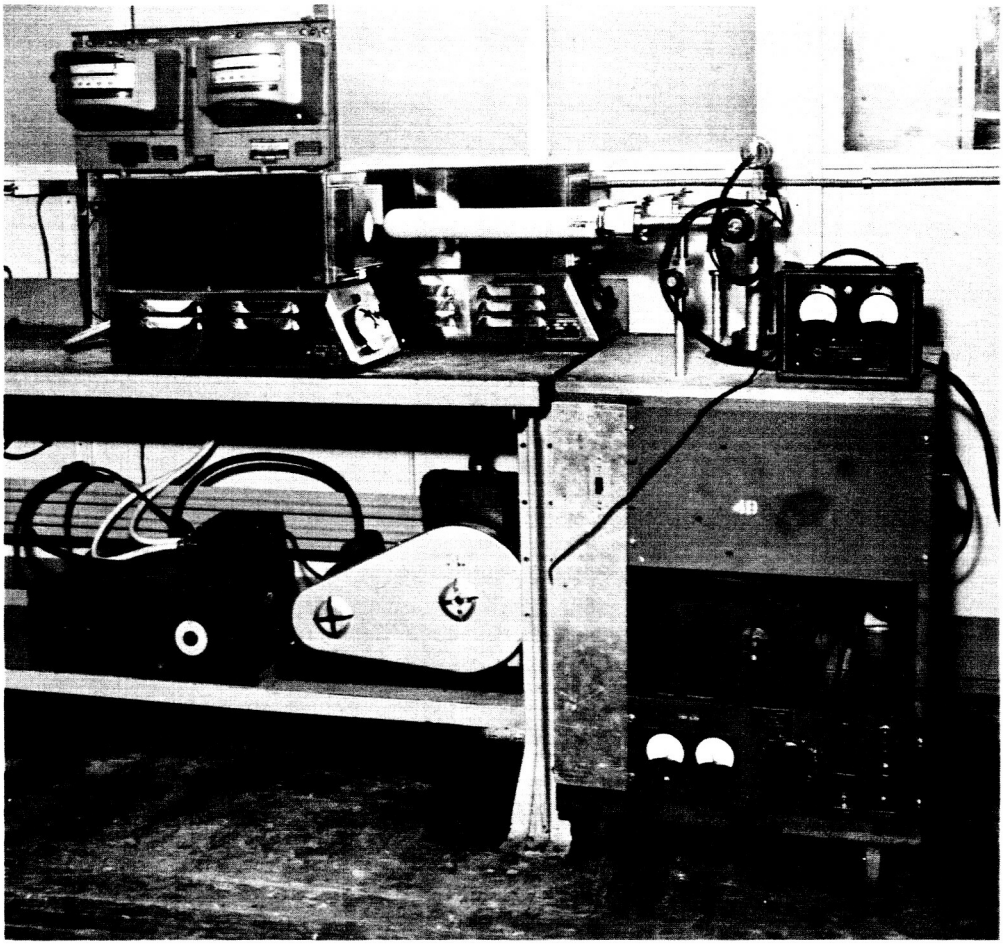

Figure 2 - Ceramic Seal Evaluation Test System

a. ACTIVE ALLOY TEST SEAL

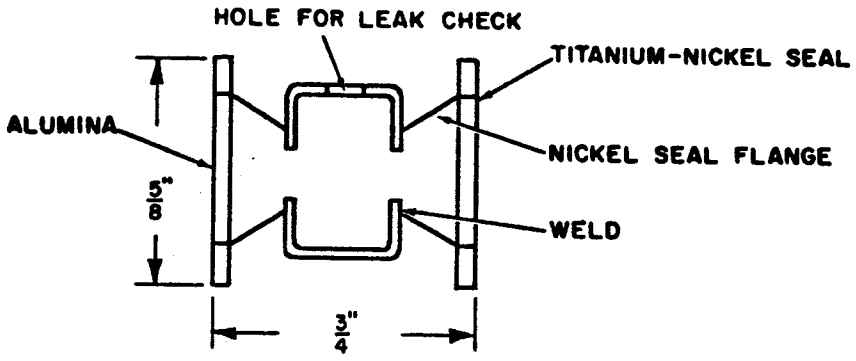

b. METALLIZED SEAL TEST SAMPLE

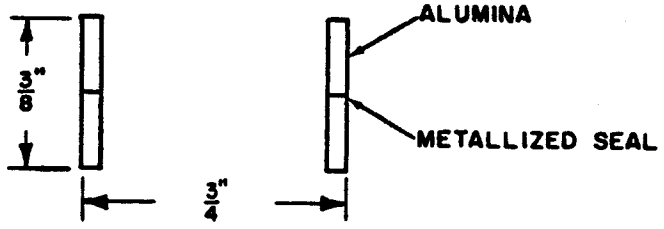

Figure 3 - Schematics of the Types of Ceramic Seals Being Tested During This Program

1500°C and below, the bond at the ceramic interface becomes questionable. All subsequent seals tested were metallized at 1560°C. The braze materials evaluated included copper-gold, gold-nickel, and palladium-cobalt. The copper-gold samples were divided into two groups, (1) 97% alumina body, and (2) the 94% alumina body.

Groups 1 and 2 of the copper-gold brazed seals accumulated a maximum of 3730 hours and the gold-nickel and palladium-cobalt brazed seals accumulated 2820 hours. After approximately 900 hours the oven containing the latter samples malfunctioned. During this excursion the oven temperature exceeded 1200°C. At this time one of the nickel-gold seals developed a leak.

Figure 4 is a photograph of five seals after 2150 hours. The three samples to the right are nickel-titanium seals, and the two on the left are metallized copper-gold seals.

Results of these extended tests indicate that both the active-alloy enriched nickel, nickel-titanium seals and the metallized seals could be used for seals operating up to 800°C. The copper-gold, however, becomes questionable at temperatures exceeding 800°C for extended periods because of their relatively high evaporation rate. Test diodes fabricated during the course of this program did utilize both the active-alloy and copper-gold metallized seals.

THYRATRON AND RECTIFIER TUBES

Problem Delineation

The work effort in the area of high-temperature rectifier and thyratron tubes consisted of a study of the basic problem areas in the development of tube designs capable of operating under environmental conditions of high temperature and high vacuum. The major problem areas confronting the successful development of both rectifier and thyratron tubes for high-temperature (800°C) operation are:

1) ceramic-metal seals
2) cathodes
3) back emission from the anode
4) grid emission
5) electrode sputtering and gas clean-up

Hot cathode gas rectifiers and thyratrons are generally capable of high-current, high-voltage operation. The thyratron differs from the

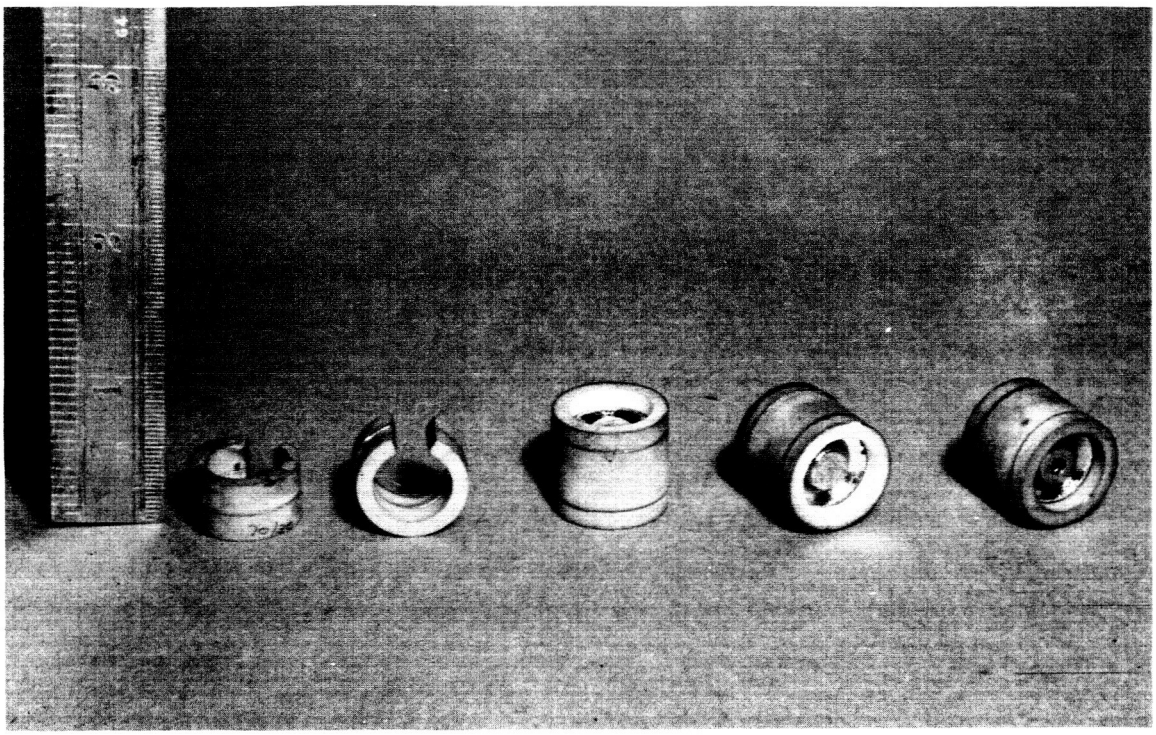

Figure 4 - Ceramic Seal Evaluation Samples

gas diode only in the starting mechanism. Once the discharge has been started in a thyratron by the grid pulse, the tube current is controlled by the impedance of the external circuit. After the grid has fired it becomes surrounded by a positive ion sheath which shields the grid from the plasma. Any change in the grid potential only changes the sheath thickness without influencing the main discharge characteristics. The tube regains control only after the anode voltage has been driven negative for a long enough time to allow the residual ionization to decay to a point where the field due to the grid potential can extend into the cathode region. The deionization time or recovery time of a given tube structure determines the operating frequency. The recovery time in general depends on the gas pressure, tube current, electrode distance, and grid potential. For short recovery times for inverter applications, the electrode distances and grid structure are made small to shorten the ion diffusion times.

In a hot cathode discharge operating in the space-charge-limited condition, a double sheath forms in front of the cathode, i.e., a negative sheath is adjacent to the cathode and a positive ion sheath is joining the plasma. This is termed the Langmiur mode. If the circuit impedance is lowered, thereby increasing the current so that cathode operation is temperature-limited, a single positive ion sheath forms in front of the cathode, causing an increase in the cathode fall of potential. Any additional increase in current may result in arc spots forming on the cathode surface, resulting in excessive cathode sputtering and stripping of the cathode surface. This is caused by ions accelerated through the cathode fall.

Dispenser-type cathodes have an advantage over the typical oxide-coated cathode in that the emission characteristics are not permanently changed by this process, since the emissive material is replenished from the bulk cathode. The main disadvantages with a dispenser cathode are the relatively high evaporation rate and the high heater power necessary to obtain the operating temperature. Evaporants, principally barium and/or barium oxide, lower the work function of the other tube electrodes causing back emission from the anode and grid emission at the elevated temperatures. At operating temperatures above 400°C, emission from the anode and grid can become appreciable, resulting in the inability of the tube to hold off inverse voltage and, in the case of the thyratron, causing loss of grid control.

Two approaches to the successful development of high-temperature tubes which warrant investigation are: (1) the use of a barium cathode system with the anode and grids operating at temperatures high enough to

prevent evaporants from remaining on the anode or grid surfaces (above 900°C), and (2) the use of a less efficient cathode system such as the thoriated tungsten cathode with the anode or grid operating at a relatively low temperature (less than 900°C). The cathode efficiency here is defined as the emission current in amperes per watt of heater power.

Figure 5 is a plot of the saturated emission density (I_s) as a function of temperature for several types of cathodes. Curves 1, 2, 3, and 4 represent typical emission characteristics of the oxide-coated cathode, barium-calcium-aluminate-tungsten matrix cathode, thoriated tungsten cathode, and metallic tungsten cathode, respectively. The dotted curves represent the ratio of saturated emission per watt of radiated power (P_r) at any given temperature. These curves are only approximate since a value of 0.25 for the total emissivity was used for purposes of comparison. The efficiency curves represent only the power lost by radiation from the cathode surface. The actual efficiencies are somewhat less than this when conduction and electron cooling losses are considered. The thoriated tungsten cathode does not become efficient until a temperature on the order of 2000°K (1727°C) is reached, whereas the barium cathode shows approximately the same efficiency at 1200°K (927 °C).

Considering the first approach, the adsorption of barium-on-tungsten exhibits mainly the same phenomena that is observed with the cesium-on-tungsten system as described by the Langmuir-Taylor curves[1]. Becker[2] shows the emission current of the tungsten-barium system as a function of θ, the fraction of the surface covered with barium. This suggests the possibility of operating a barium cathode in a device where the anode and grid are operated at such a temperature that a low barium coverage is maintained. This mode of operation requires a choice of anode and grid material which has a high barium evaporation rate. Titanium has been used quite extensively as a grid material for operating temperatures up to about 400°C to 500°C. For higher temperature applications carbon or pyrolytic graphite would appear to be a better choice of material. Figure 6 shows the change of emission with time for carbon-coated molybdenum after barium oxide was evaporated onto the surface. The curves indicate a rapid decay in emission at temperatures above 950°C.

(1) I. Langmuir, and J. B. Taylor, The Evaporation of Atoms, Ions, and Electrons from Cesium Films on Tungsten, Phys. Rev., 44, 423 (1933).

(2) J. A. Becker, The Use of Thermionics in the Study of Adsorption of Vapors and Gases, Trans. Faraday Soc., 28, 148 (1932).

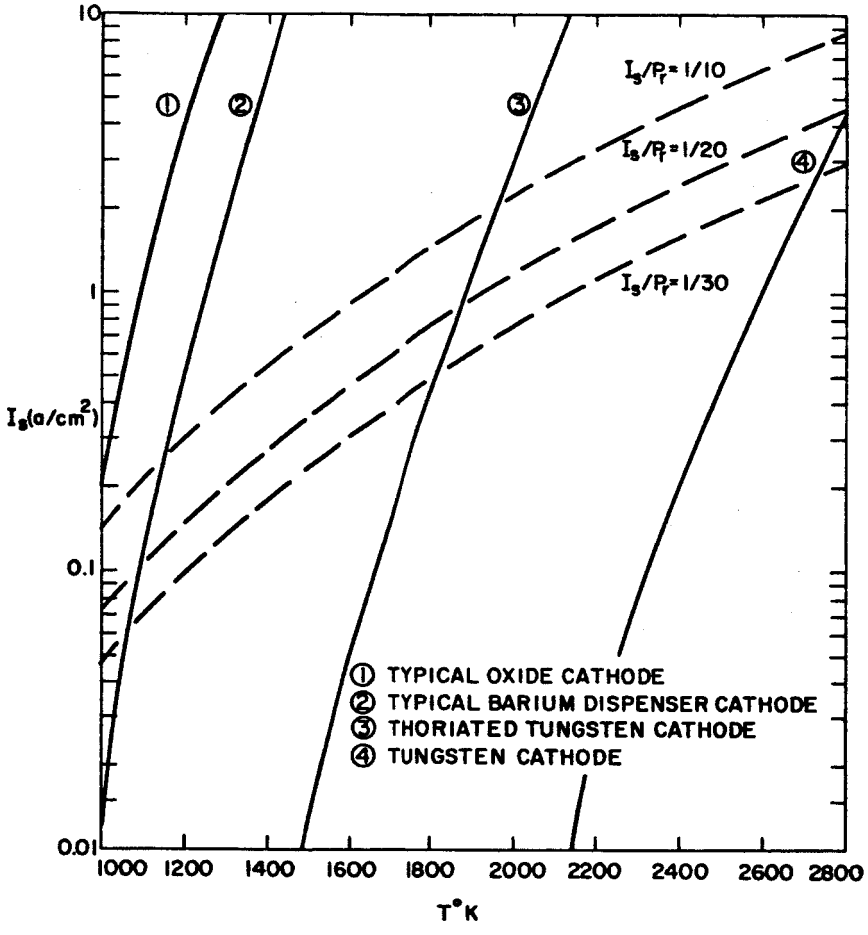

Figure 5 - Saturated Emission Density as a Function of Operating Temperature for Several Types of Cathode

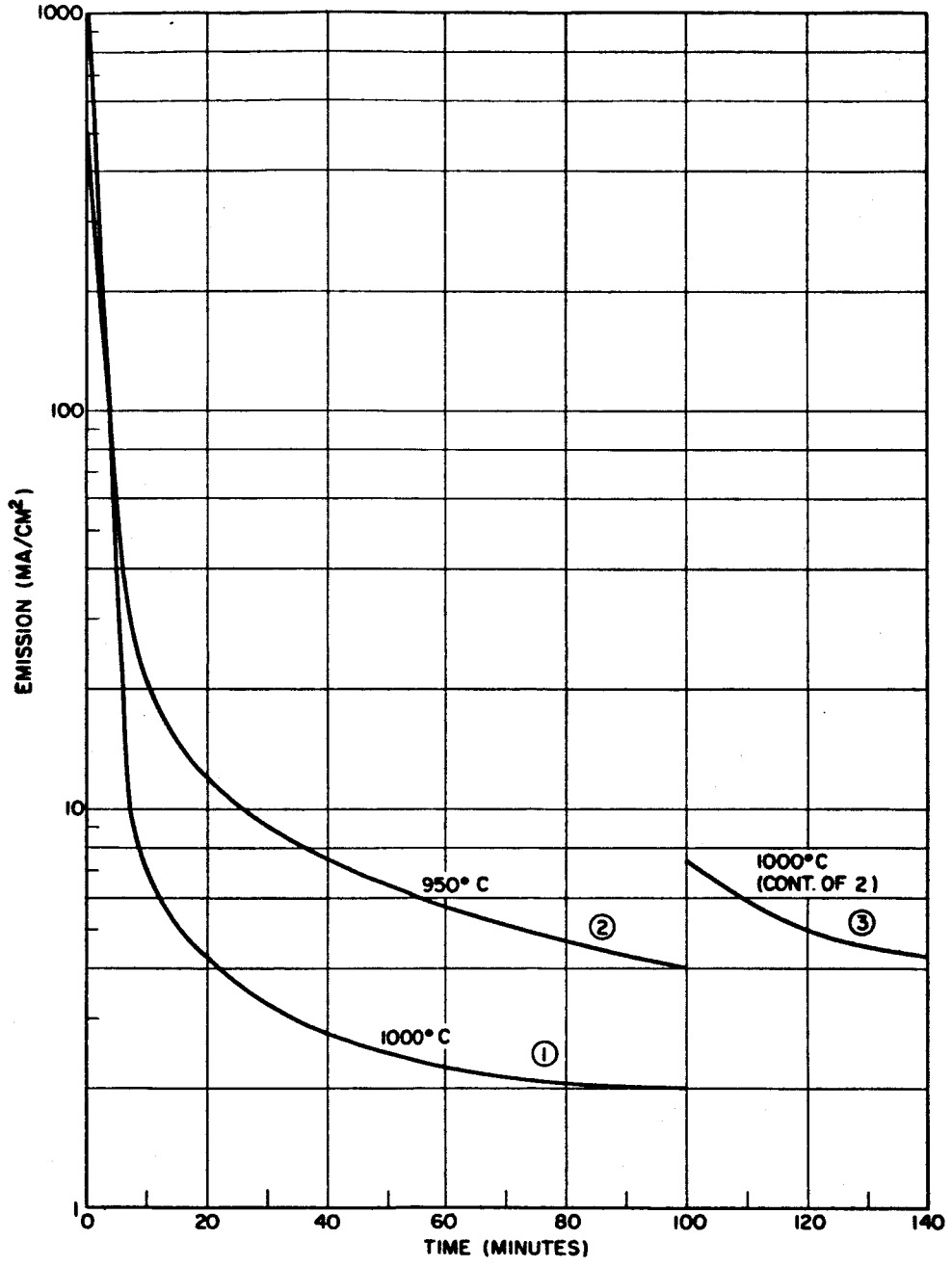

Figure 6 - Change in Emission vs Time for Carbon-coated Molybdenum After Barium Oxide is Evaporated on the Molybdenum

The use of a low-efficiency cathode (such as a thoriated tungsten cathode) for high-temperature tube operation is a second approach to maintaining low back emission from the anode and low grid emission. In this case, the evaporation of thorium to the other tube electrodes would not be expected to result in serious back emission problems. Figure 7 shows the emission density from the thorium-on-tungsten system for the case of optimum coverage and for the case where the thorium coverage is half that of the optimum coverage. Experimental evidence given by Danforth for the deactivation of a monolayer of thorium by evaporation shows that no appreciable deactivation occurs below a brightness temperature of 1600°C. However, as shown in Figure 7, even at optimum thorium coverage the emission density is on the order of 1 ma/cm^2 at 1000°C brightness. Between 800°C and 900°C, the current density is estimated to be in the range of 10^{-6} amperes/cm^2. For less than optimum coverage, emission densities of 10^{-7} amperes/cm^2 would be expected. The main disadvantage with this approach is the high cathode temperature required. Temperatures on the order of 1950°K (1677°C) to 2000°K (1727°C) are necessary to obtain emission densities of from 3 to 5 amperes/cm^2. This requires relatively high heater power necessitating either high filament current or high filament voltage. In gas tubes the filament voltage drop becomes an important parameter since breakdown can occur across the filament if the voltage exceeds the breakdown potential in the cathode region. Generally, the maximum filament voltage should be kept below 10 volts and most commonly on the order of 5 volts. For this reason it was decided to base the initial investigations on the barium system.

Gas Clean-Up

The term gas clean-up denotes the loss of gas in a gas discharge device. Causes include chemical, mechanical, or electrical processes. Chemical clean-up occurs as a result of reactions between the gas and internal structures. This is generally not of concern in inert gas devices except where electrochemical reactions might occur with nitrogen. Mechanical processes can also occur -- an example being the occlusion of the gas into metal parts. The major cause of gas clean-up of the inert gases, however, can be termed as electrical. One type of electrical clean-up occurs when ions, as well as gas atoms, become trapped on the tube structures during application of inverse voltage. Ions can be taken up in the electrode itself or trapped on the walls of the tube. Trapping is due to sputtered material from the anode. This method of gas clean-up is used in the "evapor-ion" or "vac-ion" pumps. Titanium is generally used as the cold cathode because of its relatively high sputtering yield.

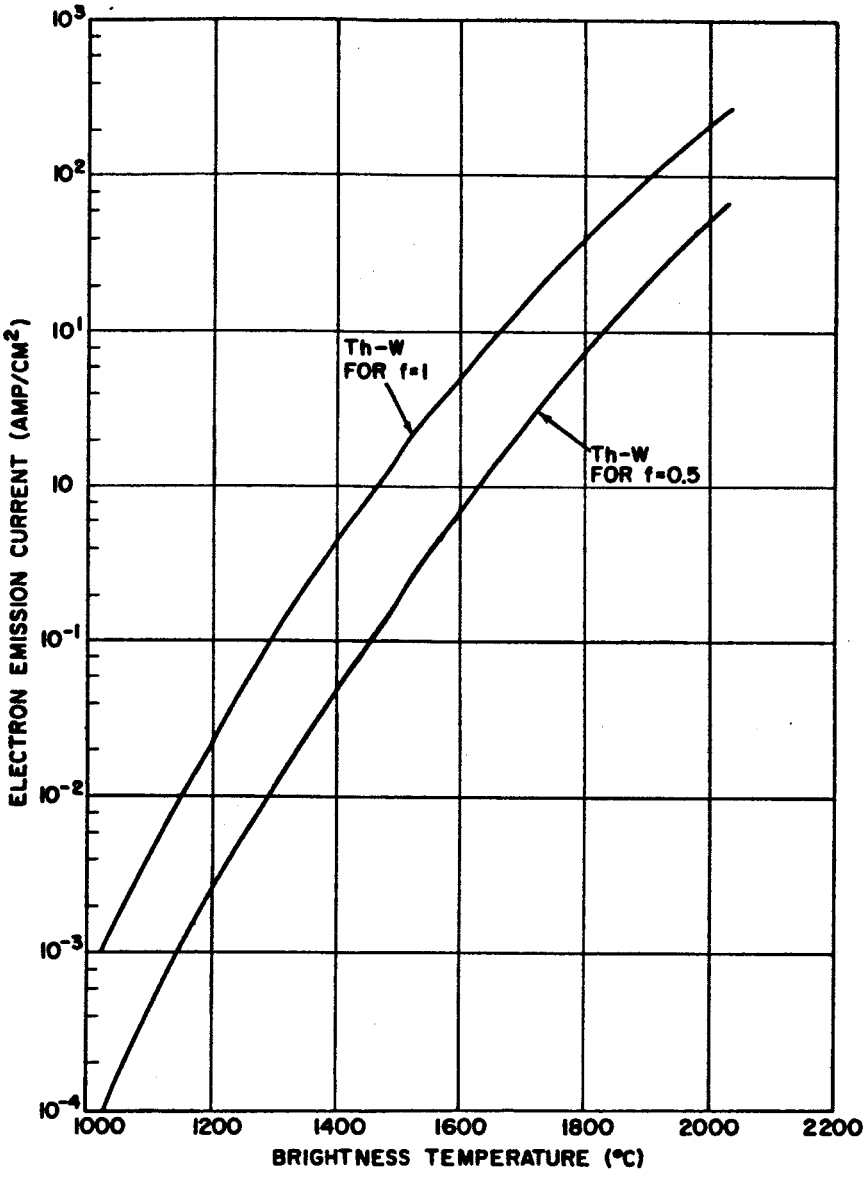

Figure 7 - Emission Density as a Function of Brightness Temperature for a Thorium-on-Tungsten System

The ratio of captured gas to evaporated metal can be as high as 0.5 gas atoms/atom of sputtered metal[3].

Ion bombardment and the resultant sputtering become a limitation insofar as frequency of operation of gas discharge devices is concerned. When the rate of rise of inverse voltage is rapid enough so that large numbers of ions are accelerated to the anode, sputtering of the anode surface takes place and results in gas clean-up. The clean-up rate in gas diodes and thyratrons depends on the degree of ionization at current cessation and on the rate of application of inverse voltage. This relationship is expressed as:

$$\text{commutation factor CF} = (dv/dt) \times (di/dt)_o$$

The (dv/dt) term defines the rate of rise of voltage immediately after current cessation (commutation) and $(di/dt)_o$ is the rate of decrease of current just prior to commutation. This is a measure of the degree of ionization. As the frequency of operation of a thyratron is increased, the level of ionization at current zero becomes greater, and, therefore, increases the gas clean-up rate. Typical industrial-type gas thyratrons designed for 5,000 to 10,000 hours life have CF factors on the order of 120 to 200. The severity of clean-up depends a great deal on the particular tube application as related to current and voltage wave shapes.

Another factor influencing the clean-up rate is the sputtering of anode material. For comparison purposes reference is made to Figures 8 and 9. Carbon has been found to have about the lowest sputtering yield in noble gas discharges. Because of this and other desirable properties, carbon becomes a good candidate as an anode and grid material for high temperature tubes.

Anode Emission and Grid Emission

Factors Involved

Adsorption of evaporants from the cathode on the anode and grid structure of a diode or thyratron decreases the work function. Under operating conditions where the anode and grid temperature can be kept cool, lowering of the work function does not present any serious control

(3) Saul Dushman, Scientific Foundations of Vacuum Technique, 2nd edition, revised by members of General Electric Research Laboratory, edited by J. M. Lafferty (Wiley, New York, 1962).

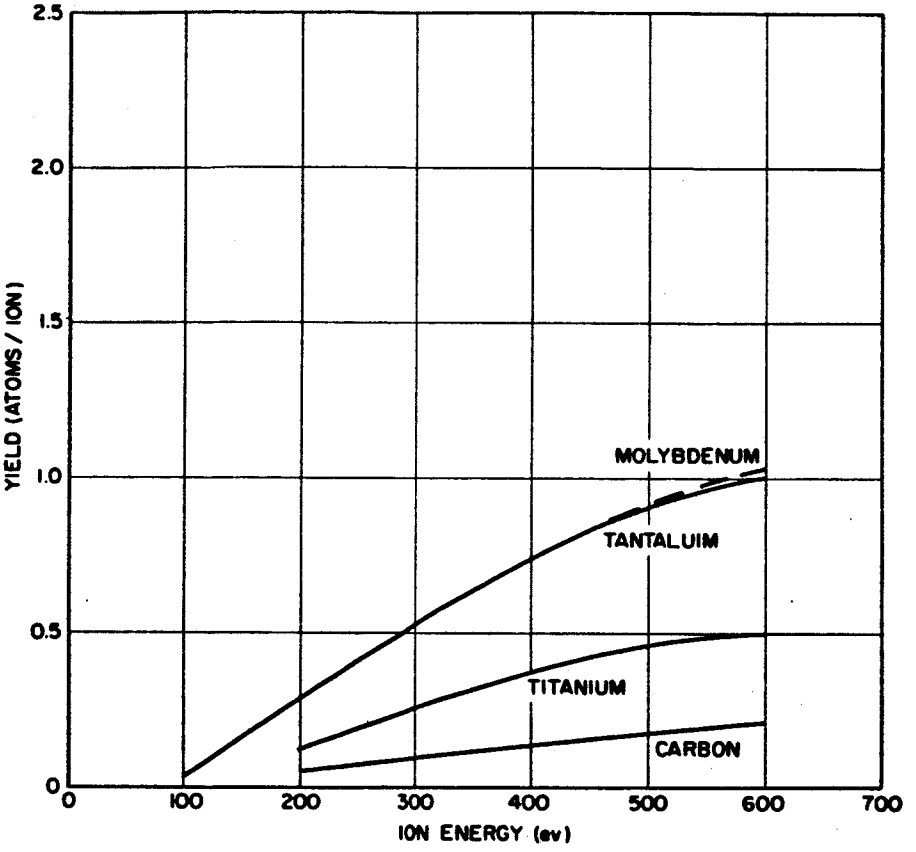

Figure 8 - Sputtering Yields in Xenon

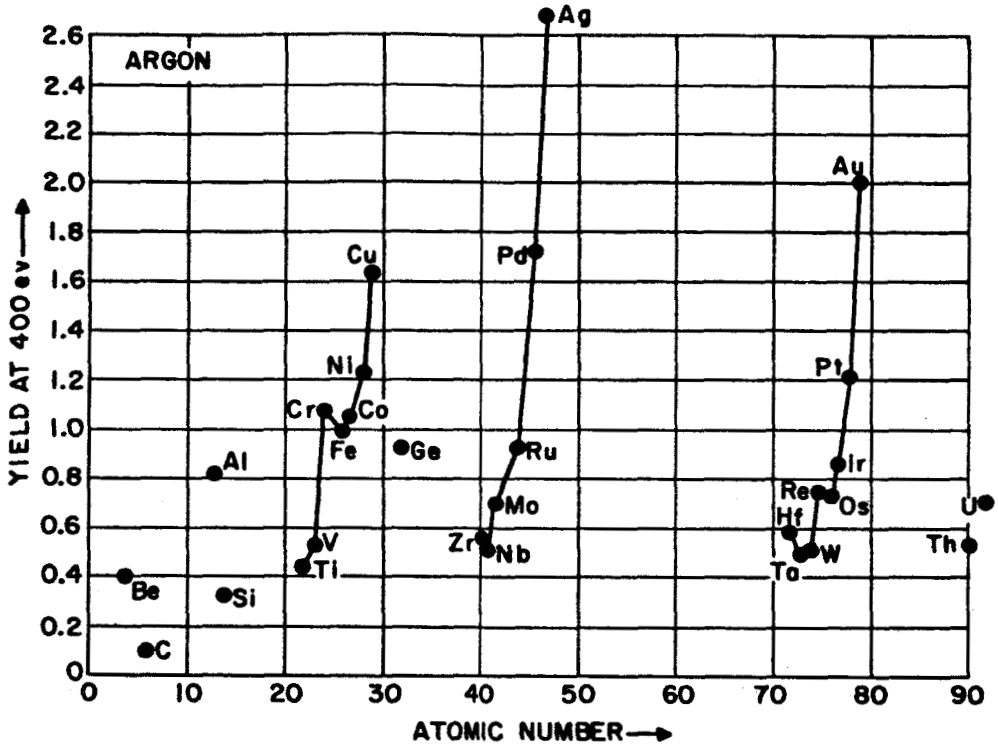

Figure 9 - Sputtering Yields at 400 ev Argon Ion Energy for 28 Elements versus the Element's Atomic Number (N. Laegried and G. K. Wehner, J. Appl. Phys., 32, 365 (1961).)

problems. However, at temperatures in the 500°C and higher range, emission from these low work function surfaces can cause discharge current to flow, resulting in back emission from the anode and inability to hold off inverse voltage. In a thyratron, excessive grid emission results in loss of grid control. The cathode therefore becomes a critical element in high-temperature, high-current tubes not only from the standpoint of emission density but also from an evaporation rate aspect. The work function reduction of the auxiliary electrodes depends on the net arrival rate of adsorbant to the surface as well as the substrate material, crystographic orientation, and surface temperature. For any given surface condition, the work function of the adsorbing surface at any time is related to the fractional coverage, θ, of adsorbant. A minimum occurs in the work function corresponding to the optimum (monolayer) coverage condition. At this point θ is approximately equal to 1. The fractional coverage is a function of the net arrival rate to the adsorbing surface and is therefore dependent on the evaporation rate from the adsorbing surface, i.e.,

$$\theta = f(N_a - W_s), \quad \text{where } N_a \text{ is the arrival rate and } W_s \text{ is the evaporation rate}$$

For a given cathode operating at a fixed temperature, the incident flux to the anode or grid is essentially constant so that the θ coverage is dependent on the surface temperature of the adsorbing electrode. This is a dynamic condition in that material is constantly being evaporated to and re-evaporated from the electrode surface.

Investigations were made on the emission from various materials while continually evaporating barium from a dispenser cathode to the surface. The tests were performed in a vacuum bell-jar system where the system pressure was maintained at 10^{-7} to 10^{-8} Torr. The cathode used was a barium dispenser type cathode capable of emission densities greater than 1 amp/cm^2.

Experimental Procedure

In order to evaluate the effects of evaporants on electrode materials the evaporation rate of the cathode had to be determined. Emission measurements were then made from the adsorbing electrode while barium was continually being evaporated to surface. Approximately 200 to 300 volts was applied across the diode during the emission measurements.

The evaporation rate measurements were made using a retarding field technique[4] based on measuring the time rate of change of the anode work function caused by the deposition of evaporants from the cathode. The data obtained are the changes in voltage required to maintain a constant current through the diode. This voltage is measured continuously and the minimum of the voltage-time curve indicates a monolayer coverage of barium and barium oxide on the anode. The mass per square centimeter for a monolayer is taken to be 7.6×10^{-8} gm/cm^2. All of the evaporant is assumed to be barium.

Figure 10 shows a schematic of the bell-jar diode and Figure 11 shows a schematic of the measuring circuit. The test diode was arranged such that the cathode was mounted in a fixed position with the anode mounted on a movable arm which could be rotated by means of an external magnet. The cathode-anode spacing was adjusted to be between .010" to .020". The anode could be moved from under the cathode, and by means of a radiation type heater, cleaned prior to each measurement. The anode could be removed and another of different material inserted. Figures 12A and 12B are photographs of the bell-jar with the anode under the cathode and away from the cathode. The complete system is shown in Figure 13. The vacuum system consists of two sorption pumps and a Varian 40 liter/sec vac-ion pump. A Keithley 604A electrometer was used to measure the change in voltage with the output fed into a Varian strip chart recorder.

The same experimental set-up was used to measure the back-emission from various anode and grid materials. For these experiments the dispenser cathode was operated at a fixed temperature to keep the arrival rate of evaporants constant. Voltages of 200 to 300 volts were applied across the diode with the cathode negative. The electrode temperature was varied so that the electron emission could be observed over the temperature range of 300°C to 1200°C.

Initially, to check the technique for measuring evaporation rates, the results using a barium orthosilicate dispenser cathode were compared to evaporation rate measurements made on similar cathodes using the X-ray emission method for quantitatively measuring the amount of barium evaporated. The results shown in Figure 14 show good agreement between the two methods. A similar curve for a high emission density cathode

(4) J. V. Florio, Retarding Field Technique for Measuring Sublimation from Dispenser and Oxide Cathodes, J. Appl. Phys., 34, 200 (Jan. 1963).

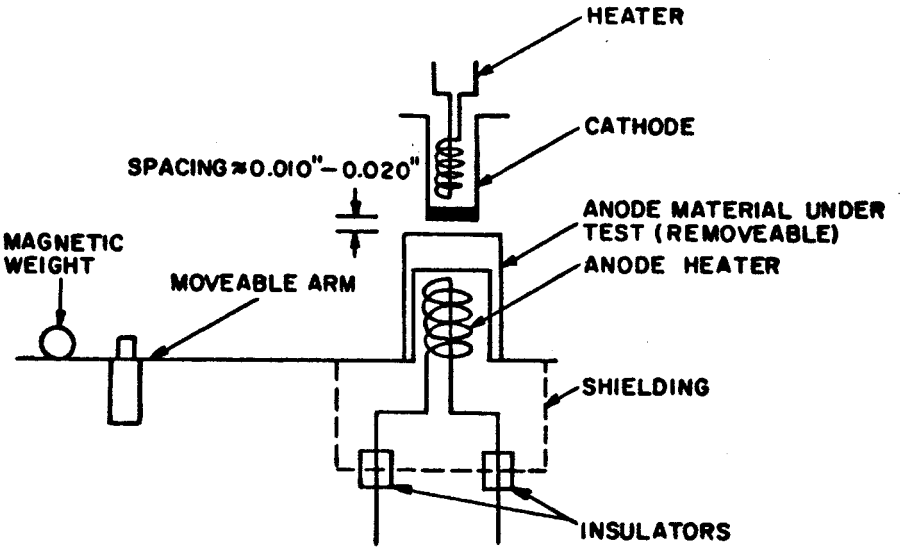

Figure 10 - Schematic of the Bell-jar Diode

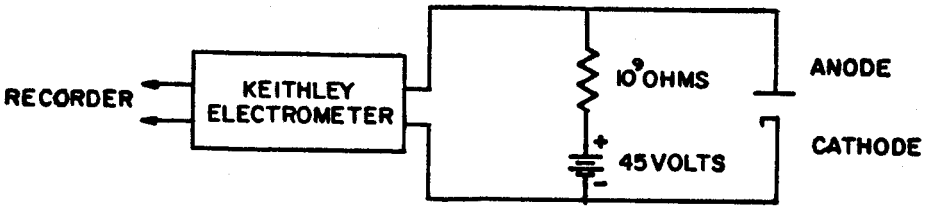

Figure 11 - Schematic of the Measuring Circuit

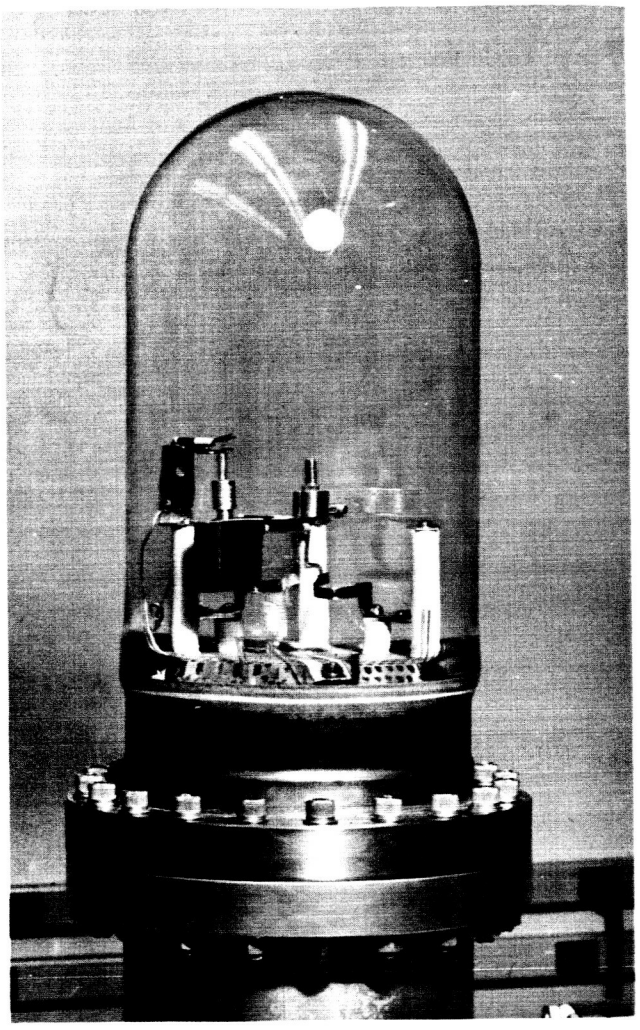

12A

(Anode under Cathode)

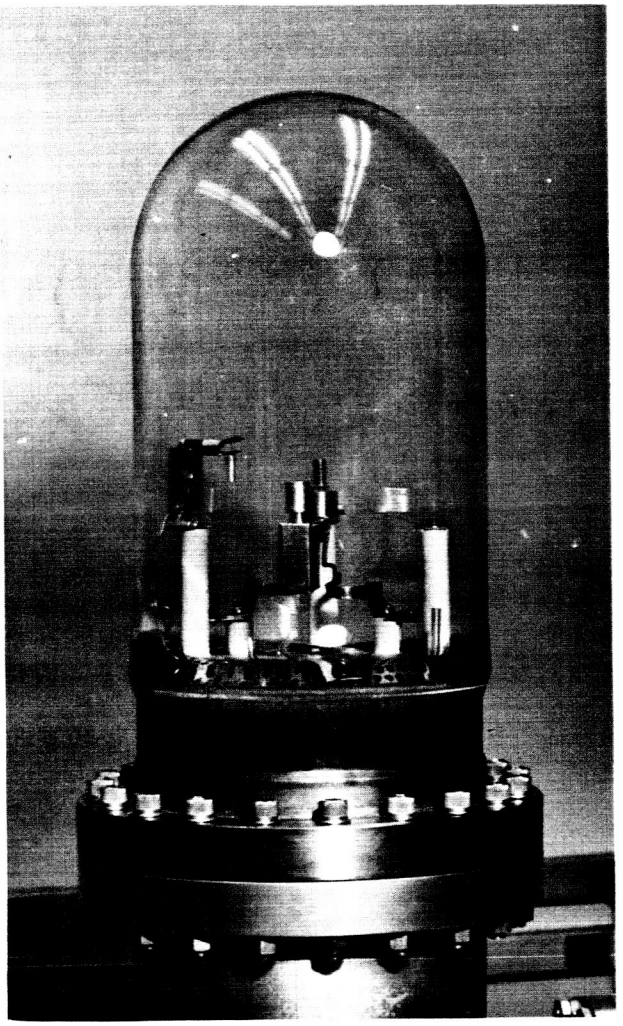

12B

(Anode Away from Cathode)

Figure 12 - Bell-jar System for Cathode and Anode Evaluations with Movable Anode

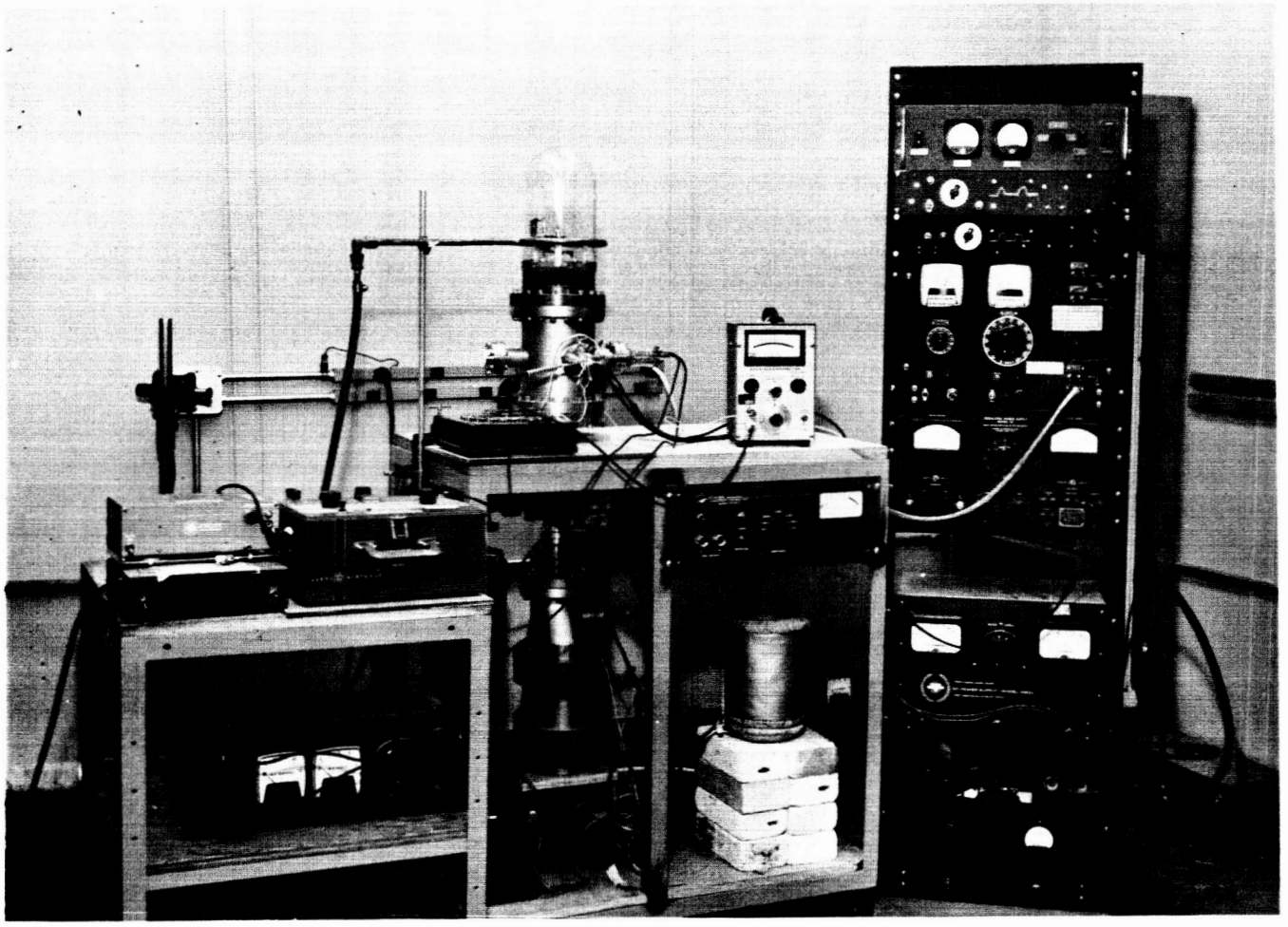

Figure 13 - Bell-jar Test System and Circuitry for Diode Test

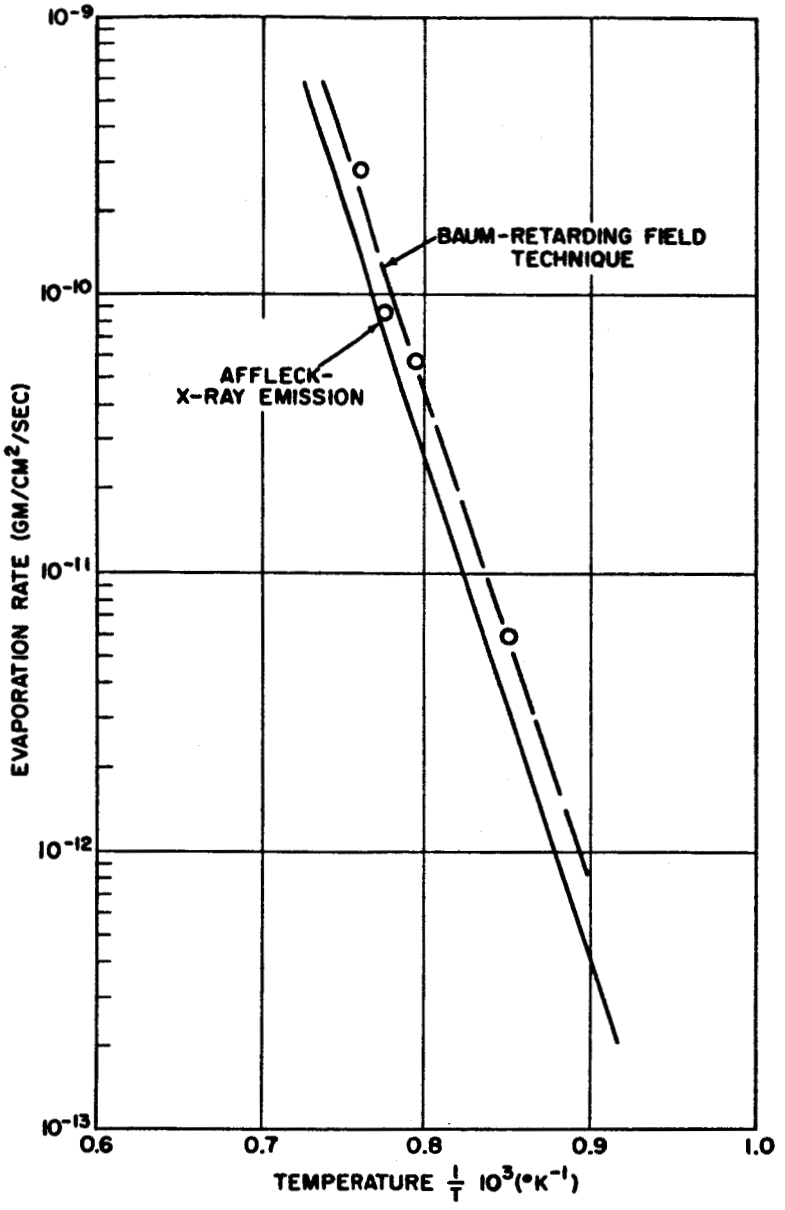

Figure 14 - Evaporation Rate of Barium as a Function of Temperature for a Barium Orthosilicate Dispenser Cathode

is shown in Figure 15. The dotted line represents the time required to evaporate a monolayer as a function of temperature. This is a General Electric Company developmental dispenser cathode which has shown current densities of 5 to 10 amperes/cm^2 over the temperature range of 950°C to 1050°C and, therefore, warrants consideration for high-power, high-temperature gas tubes.

The effects of evaporants on a titanium electrode, while constantly evaporating barium/barium oxide to the surface, showed a peak in the emission curve from the titanium at about 850°C. Above this temperature the emission decreased rapidly, indicating the evaporation rate from the titanium surface was sufficiently high so that less than optimum coverage was maintained.

Tests were also made on the emission from a porous graphite anode under similar conditions. The maximum current from the graphite was found to be on the order of 10^{-5} amps/cm^2 at 950°C, and rapidly decayed to 10^{-8} amps/cm^2. Measurements were difficult to make because of poisoning of the cathode during the reverse current measurements. This may have decreased the evaporation rate from the dispenser cathode, thus lowering the arrival rate of evaporant to the graphite surface. It was observed that cathode poisoning did not occur when the anode was at a high temperature and when current was drawn from the cathode. The poisoning occurred only when reverse current was drawn to the cathode. The cathode could be reactivated by running the diode in the forward direction for periods of 12 to 16 hours. Tests made with half-sine-wave inverse voltage (cathode position), across the diode, and with full-wave voltage showed that in both cases cathode poisoning resulted. It is believed that the poisoning results from negative ions which are generated at the porous graphite surface and then accelerated to the cathode surface when the cathode is positive.

Back emission tests were also made using an arc-cast molybdenum anode. The arrival rate of evaporant to the anode surface was 3.3×10^{-3} monolayers/sec. The results are shown in Figure 16. A maximum current of 7.5 ma/cm^2 was obtained at 925°C. The voltage across the diode was 250 volts, so the current values are essentially saturation current values.

Emission measurements from pyrolytic graphite, while continually evaporating barium to the surface, were also made. At temperatures of about 800°C and below, a gradual increase in the emission current was apparent. Maximum current levels of the order of 10^{-4} amps/cm^2 were measured at 770°C. Current levels at 900°C with the same arrival rate

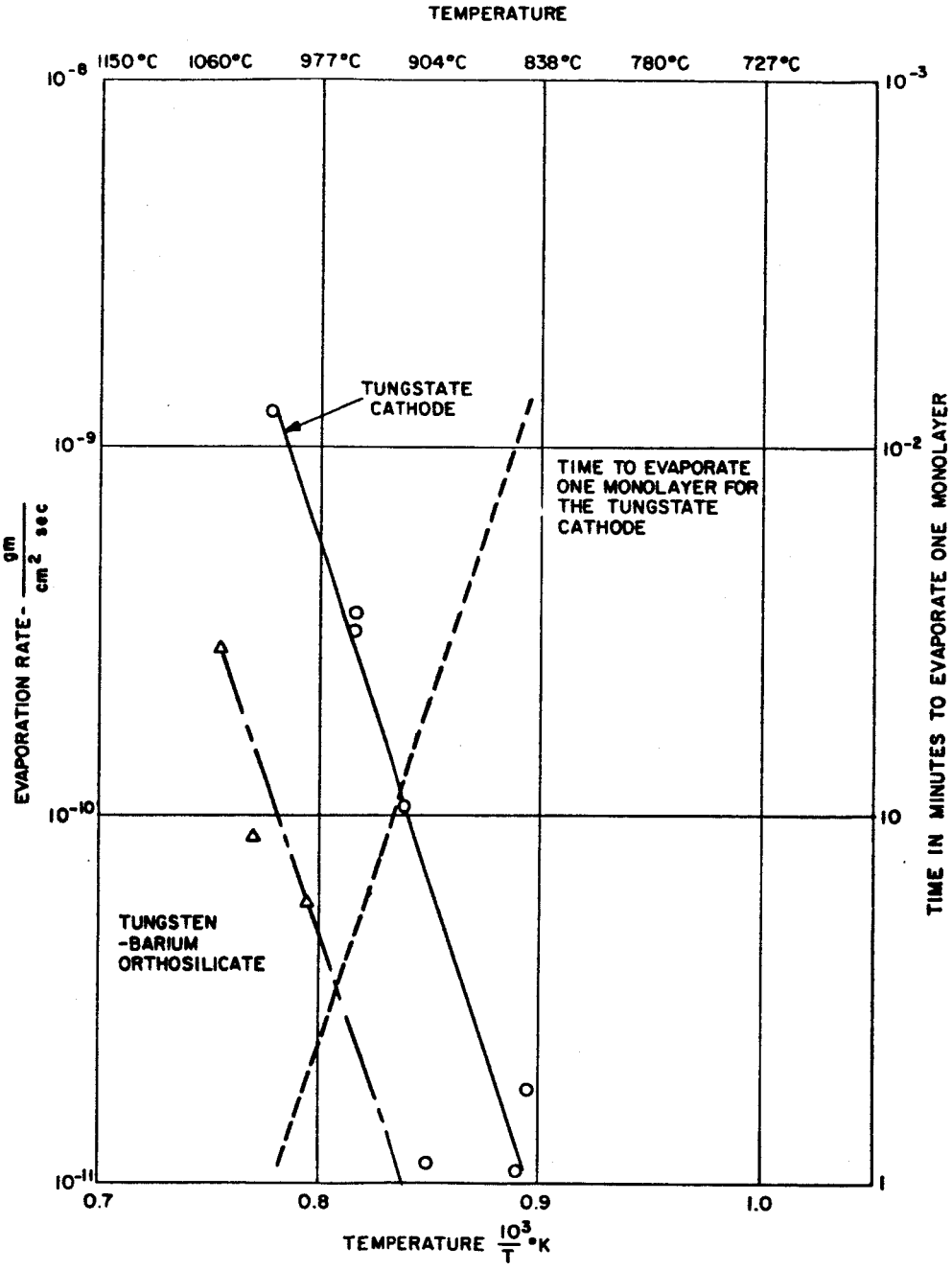

Figure 15 - Evaporation Rate Data, Tungstate Cathode

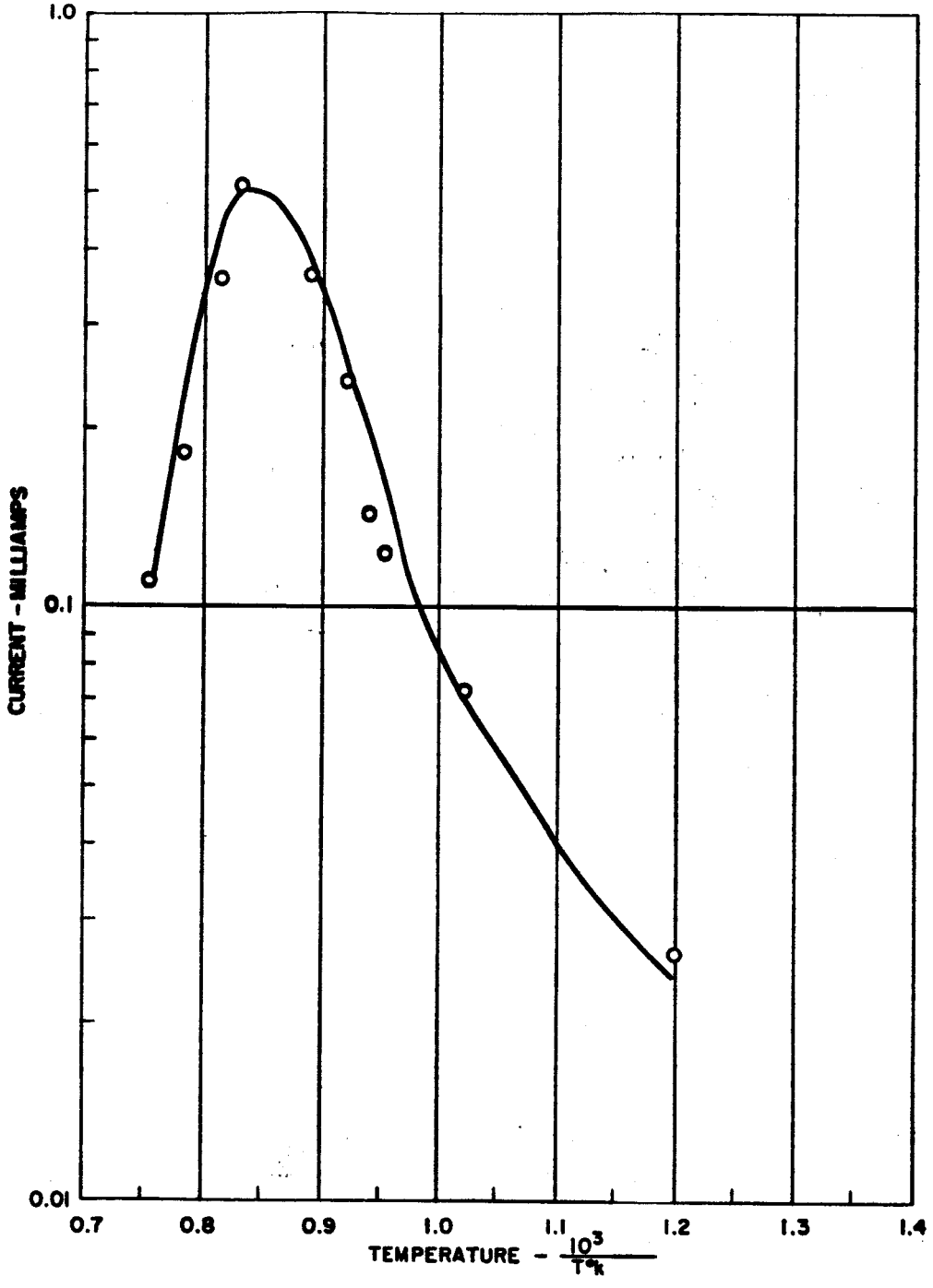

Figure 16 - Emission from Molybdenum with Barium on Surface

of barium to the surface showed a maximum emission level of 10^{-7} amp/cm^2. This is approximately three orders of magnitude lower than emission from molybdenum at the same temperature. Unlike the porous graphite anode, the pyrolytic coated graphite anode caused no cathode poisoning.

Discussion of Results

The evaporation rate measurements indicate that for barium dispenser-type cathodes the evaporation rates are probably within an order of magnitude of each other. Figure 17 is a plot of current density vs. evaporation rate for three cathode systems. The BaO on Ni represents the best data for an oxide cathode while the other two curves are for two different dispenser cathodes. Data for the barium-tungstate cathode is based on the evaporation rate data of Figure 15. Data for the barium-calcium-aluminate cathode is from the references indicated below.[5, 6] It is apparent that the best oxide cathode is the more efficient cathode; however, the emission density is limited to about 1 amp/cm^2 because of joule heating in the coating. Dispenser cathodes have the advantage of higher direct-current densities but give way in efficiency since operating temperatures are generally from 1050°C to 1100°C. The time required to evaporate a monolayer from either the oxide cathode or the dispenser cathode is short compared to the tube life. Particular attention must be given to the other electrodes regardless of which cathode is eventually used. The major advantages of specially prepared oxide cathodes are the lower temperature of operation and the subsequent lower evaporation rate. Development effort presently being pursued on the dispenser cathode, however, could make it more attractive for rugged high-current gas tubes.

The results obtained on the dynamic back emission characteristics show that pyrolytic impregnated graphite will give minimum spurious emission from the auxiliary electrodes for electrode temperatures in the desired range. In addition, graphite at 750°C to 900°C has a low sputtering yield which minimizes the gas clean-up rate. Although no data are available on the sputtering yield of pyrolytic graphite, it would be expected to have an atom to incident ion yield at least as low as the

(5) R. Levi, Improved "Impregnated Cathode", Jour. of Appl. Phys., 26, 639 (1955).

(6) I. Brodie, R. O. Jenkins, and W. G. Trodden, Evaporation of Barium from Cathodes Impregnated with Barium - Calcium-Aluminate, Jour. of Elec. and Controls, 6, 149 (1959).

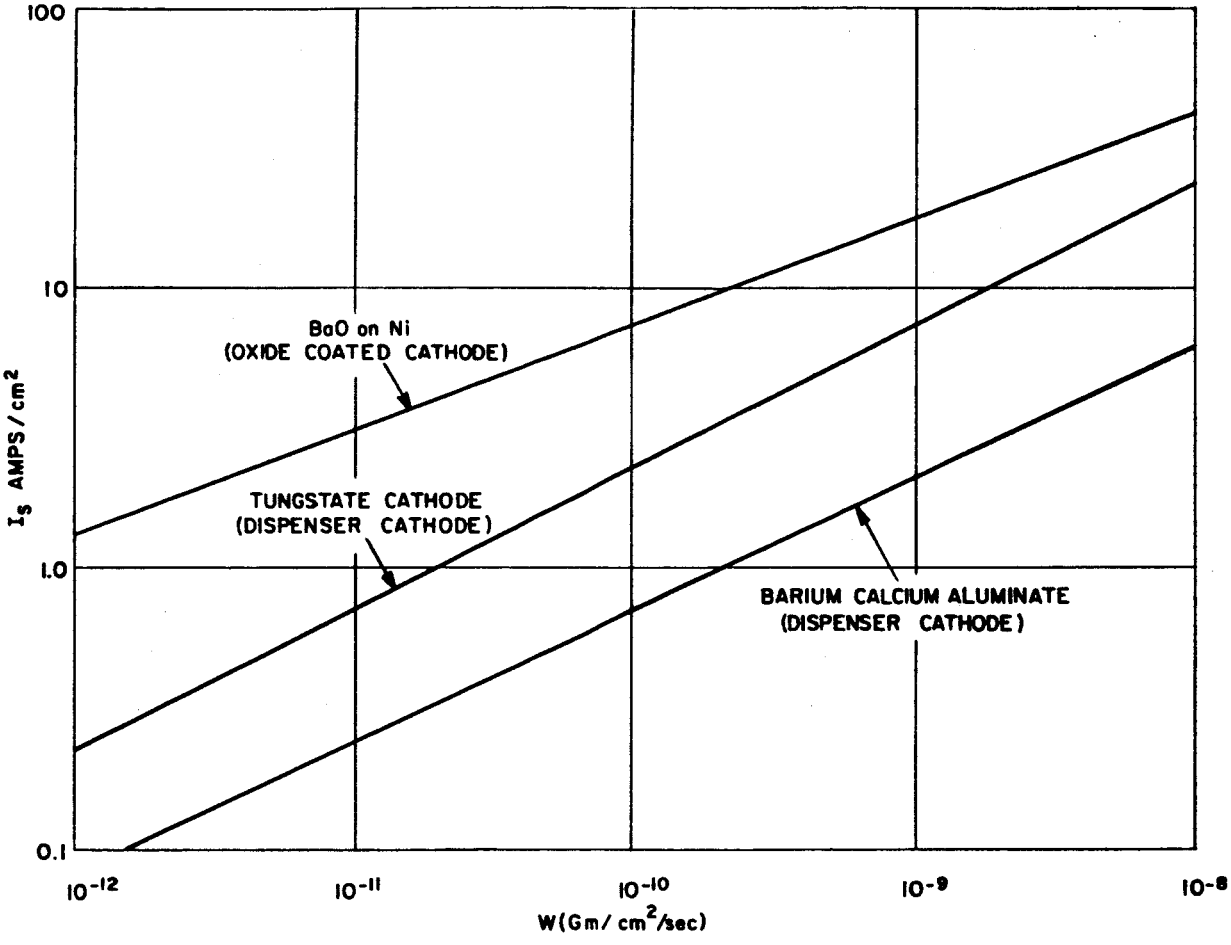

Figure 17 - Current Density versus Evaporation Rate for Three Cathode Systems

dense graphite. The use of a refractory metal, such as molybdenum, for the anode would require anode and grid temperatures approaching 1150°C .

High-Temperature Test Diode

Materials and Test Data

Based on the results just described, a test diode structure was designed and tested using both the porous graphite and pyrolytic impregnated graphite material for the anode. Tube structure is shown in Figure 18. A barium tungstate dispenser cathode was mounted on a ceramic header and surrounded by a nickel shield. A baffle was mounted over the open end of the shield cup to prevent cathode evaporants from evaporating directly to the anode. The anode was mounted on a re-entrant structure to provide some shielding to the ceramic to metal seal. A cathode header with 6 pin feed-throughs was used for the external cathode, cathode heater, and cathode thermocouple connections. The series of photographs in Figures 19 through 22 show the major sub-assemblies and the final assembly sequence (Figure 22). Figures 19, 20, and 21 show the ceramic body assembly, cathode sub-assembly, and anode assembly, respectively.

The assembled tube was mounted on the vacuum and gas loading system in a vertical position so that the tube body could be centered in a 4-inch diameter radiation oven (Figure 23). The oven consists of a four-inch diameter tungsten coil supported on ceramic spacers mounted in a tantalum cylinder. Both tube and oven were mounted in the vacuum chamber, which was pumped separately from the tubes. The tube exhaust system was valved so that the tube could be baked out while on the exhaust system. Then the tube could be cooled and valved off of the exhaust system and onto the gas loading section of the system. Xenon was loaded into the tube through a control valve at a pressure proportional to the ratio of operating temperature to loading temperature. Pressure was monitored by means of a calibrated thermocouple gauge attached to the gas loading system. Once the tube was filled to the desired pressure it could be sealed off from the system and remounted in the oven for test.

Tests were carried out at oven temperatures to 800°C and at anode voltages up to 1000 volts peak inverse. The anode supply was a variable frequency generator capable of supplying frequencies from 60 to 6000 cycles/sec. Generator output was fed into a matched transformer for voltage control. Tests were run at current levels up to about 6 amperes peak and at frequencies up to 3200 c/sec.

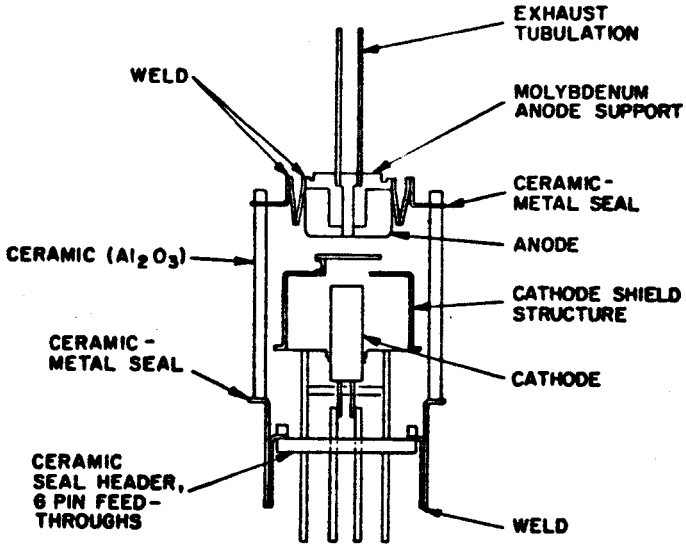

Figure 18 - Test Diode Structure

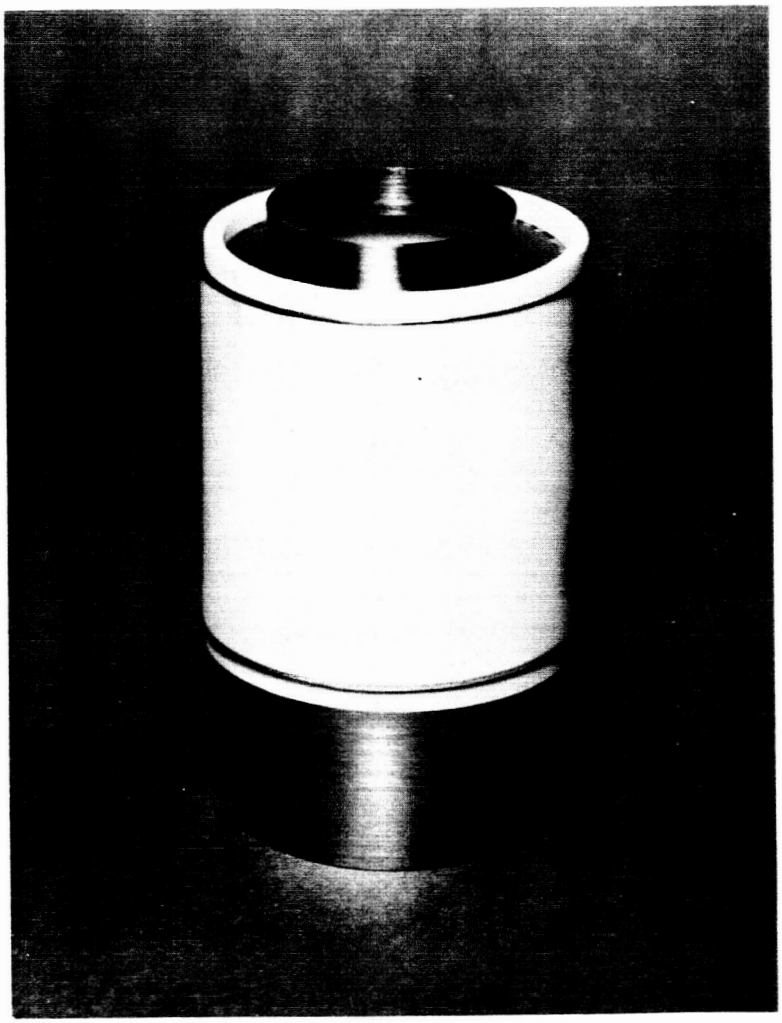

Figure 19 - Ceramic Body Assembly

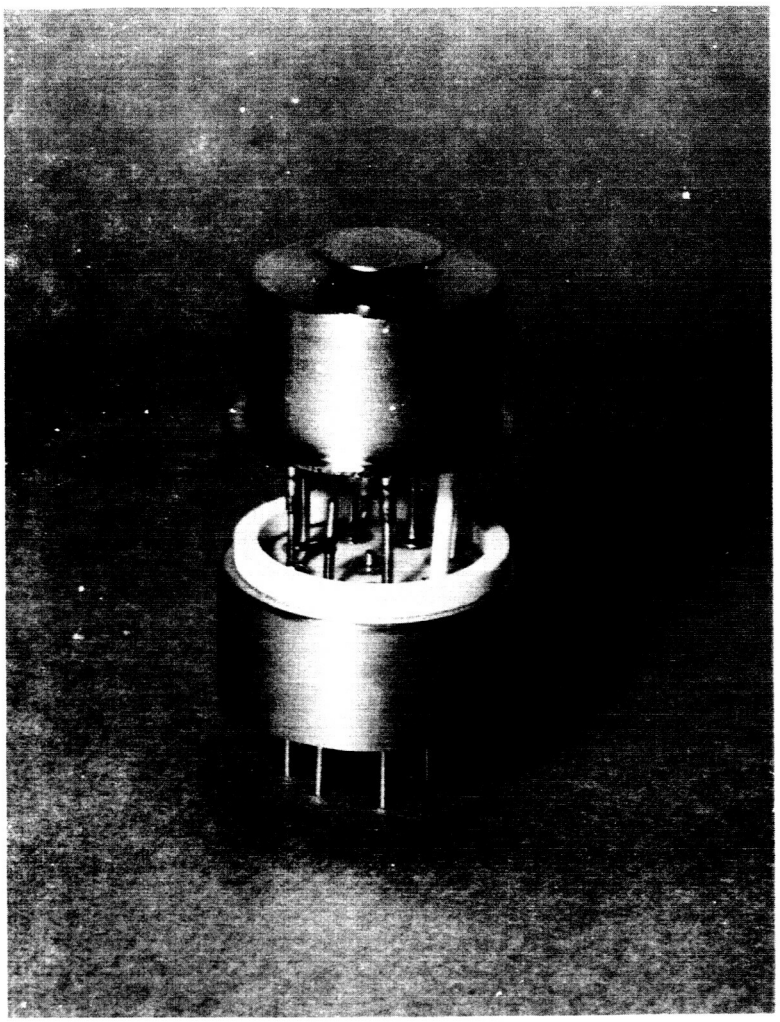

Figure 20 - Cathode Sub-Assembly

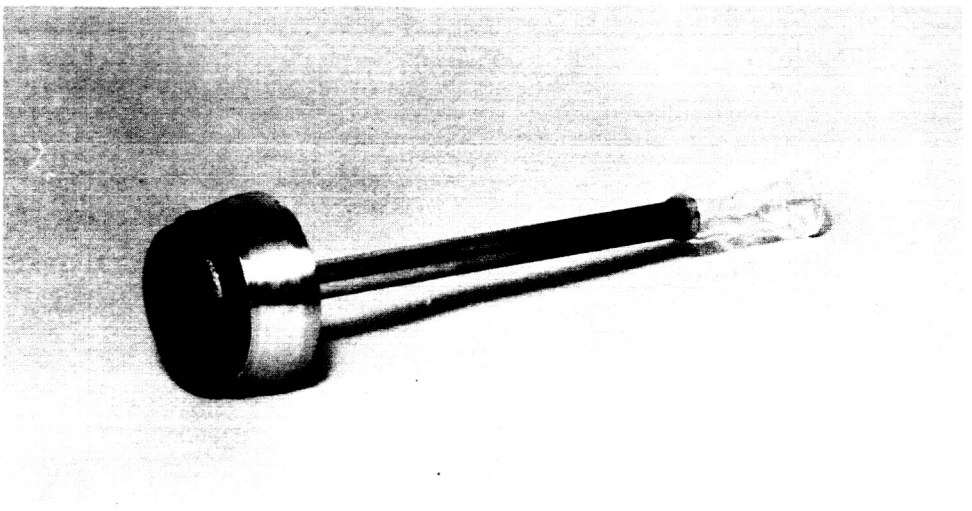

Figure 21 - Anode Assembly

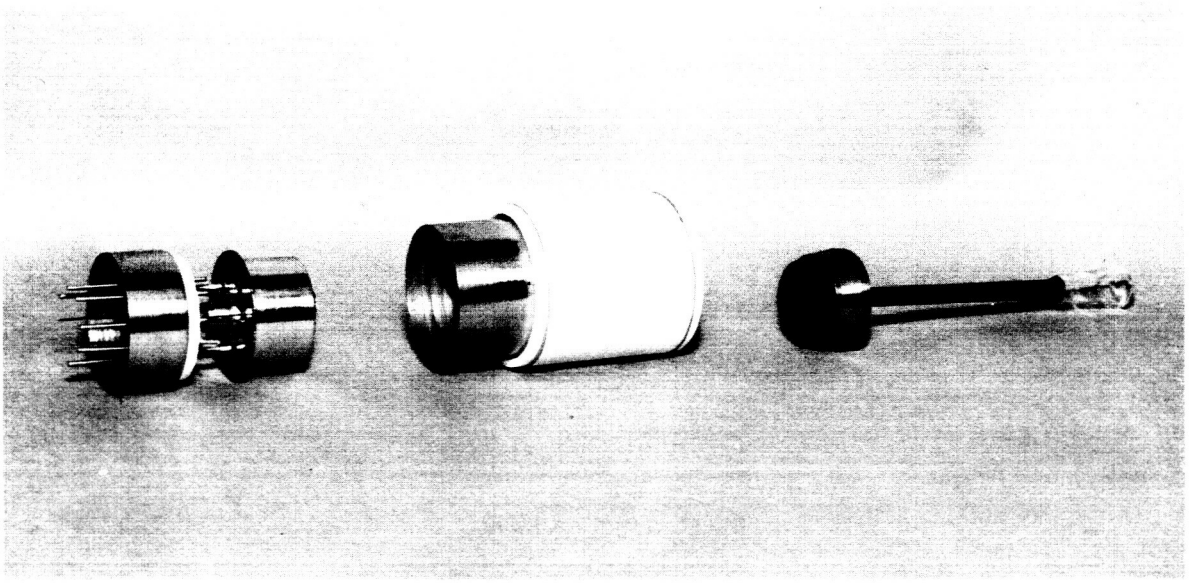

Figure 22 - Final Assembly

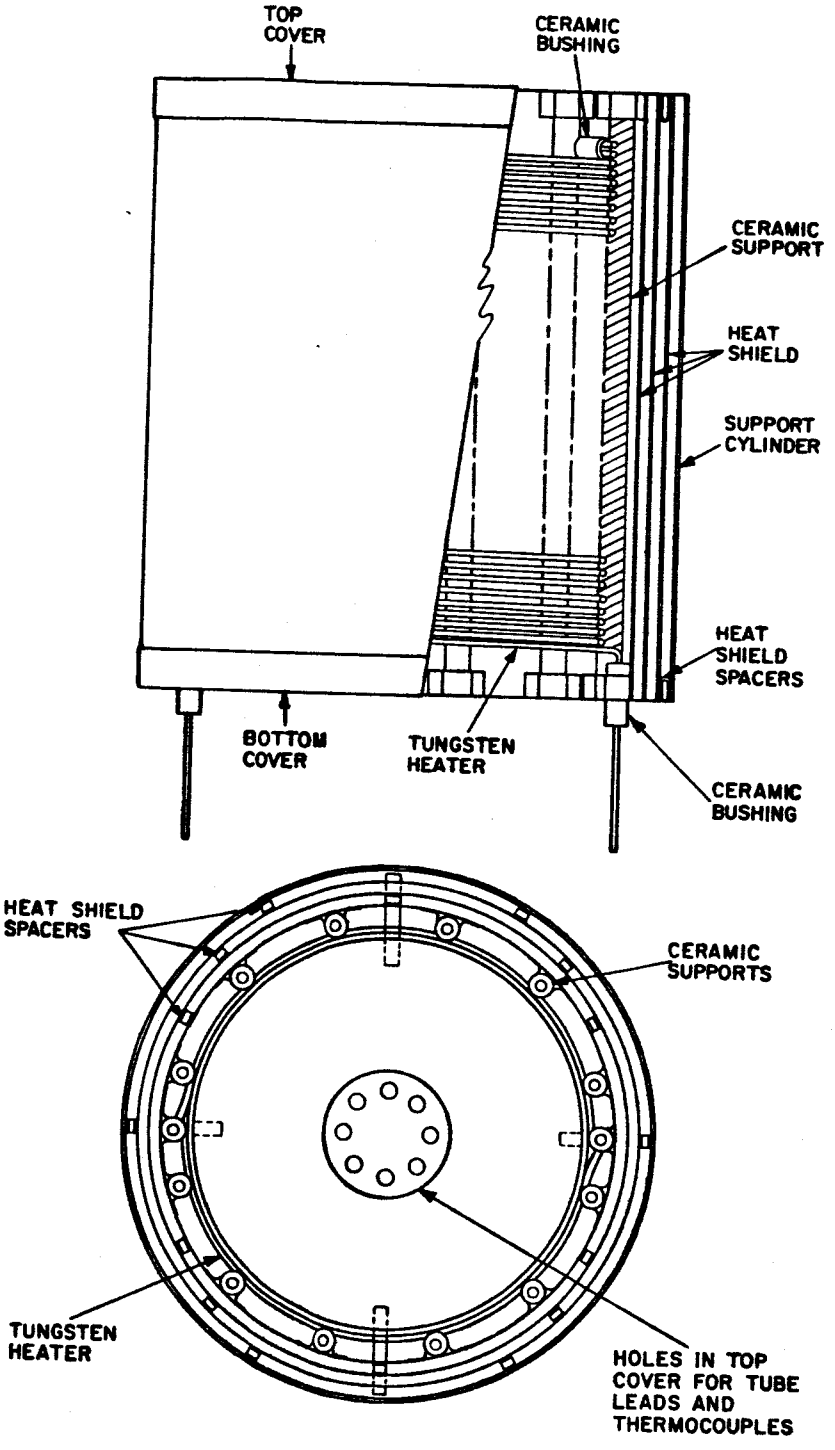

Figure 23 - Radiation Oven

Test Results

Operating data on the test diode structure are shown in Figures 24, 25, 26, and 27. Data were obtained at an oven temperature of 800°C as indicated by a thermocouple located approximately 1/4 inch from the ceramic tube wall. The operating frequencies were 400 c/s, 1000 c/s, and 3200 c/s. In all of these figures the top trace is the voltage curve, and the lower trace is the current wave. Peak current densities of 9 amperes per cm^2 were obtained in both tubes at a cathode temperature of approximately 1050°C. Some poisoning of the cathode was observed and may have been caused by gas impurities from the anode or ceramic walls. In the first diode an Arsem-fired porous graphite anode was used, and in the second structure a pyrolytic impregnated graphite anode was used. In either case no arc-backs were observed during the inverse cycle for voltages up to 1000 volts and frequencies up to 3200 c/sec. Some instabilities were observed in the inverse voltage wave beginning at about 2500 c/sec. Since these instabilities were observed in both tubes, it is believed that they were caused by circuit parameters rather than by the tubes; however, this point was not checked thoroughly. These instabilities can be seen in Figure 26 at the beginning of the inverse voltage curve. The arc-drop shown in Figure 27 for 6, 5, and 3 ampere peak currents was 10 to 12 volts. Approximately 40 hours operating time was accumulated on the first test diode and 15 to 20 hours on the second structure. In both cases, the tubes failed as a result of heaters opening because of broken weld joints where the heater was welded to the cathode.

In addition to the tube evaluations, a test was made on a revised cathode structure utilizing a porous nickel cathode impregnated with barium emission coating. This cylindrical cathode was designed to operate at approximately 850°C. At this temperature the evaporation rate of barium from the cathode is on the order of 10^{-12} gm/cm^2/sec. An emission density of approximately 0.6 amps/cm^2 was obtained. Total cathode area was 16 cm^2.

Discussion

Both tubes previously discussed were opened for inspection. An accumulation of material had built up on the cathode side of the nickel baffle of both tubes. Also, evaporated material had collected on the ceramic wall in both the anode and cathode regions. The results identifying the relative amounts of deposits by X-ray emission are shown in the following table.

400 CPS

Ambient = 800°C
Voltage Wave = 200 V/CM

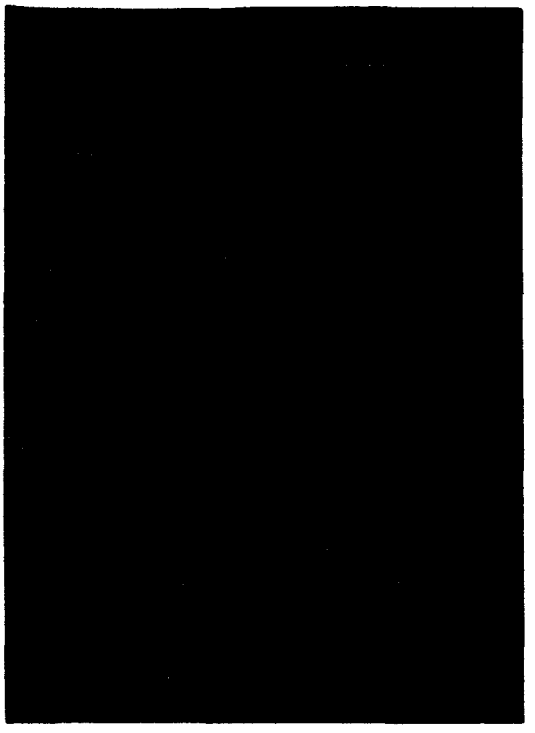

3 Amp. Peak, 1 Amp./CM

4 Amp. Peak, 2 Amp./CM

6 Amp. Peak, 2 Amp./CM

Figure 24 - Test Diode Operating Data at 400 CPS

1000 CPS

Ambient = 800°C
Voltage Wave = 200 V/CM

3 Amp. Peak, 1 Amp./CM

4 Amp. Peak, 2 Amp./CM

6.5 Amp. Peak, 2 Amp./CM

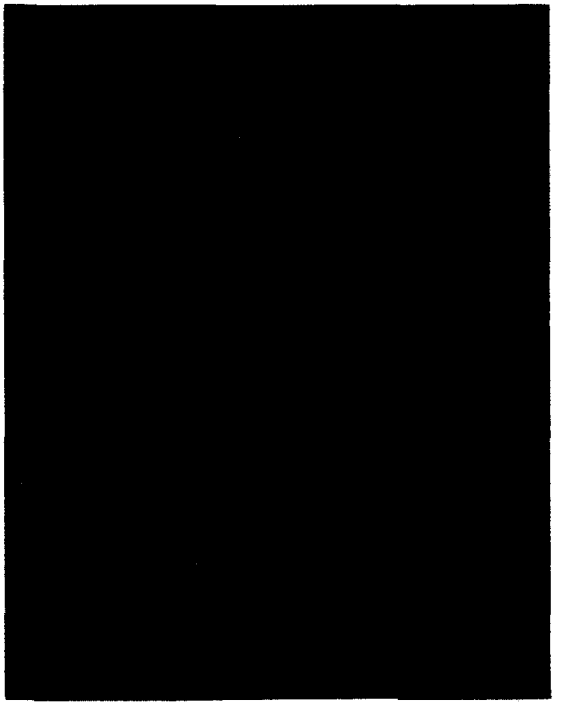

Figure 25 - Test Diode Operating Data at 1000 CPS

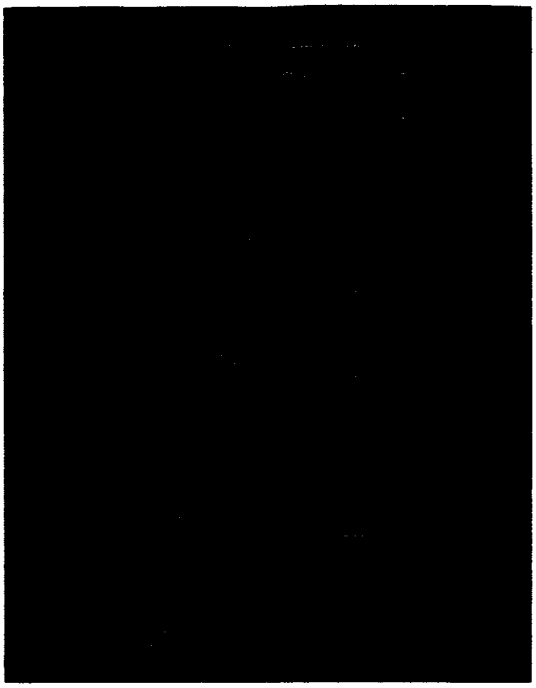

3200 CPS

Ambient = 800°C
Voltage Wave = 200 V/CM

3 Amp. Peak, 1 Amp./CM

4 Amp. Peak, 2 Amp./CM

6 Amp. Peak, 2 Amp./CM

Figure 26 - Test Diode Operating Data at 3200 CPS

Arc Drop at 3200 Cycles
6 Amp. Peak Sens. = 10 V/CM

Arc Drop at 3200 Cycles
5 Amp. Peak Sens. = 10 V/CM

Arc Drop at 3200 Cycles
3 Amp. Peak Sens. = 10 V/CM

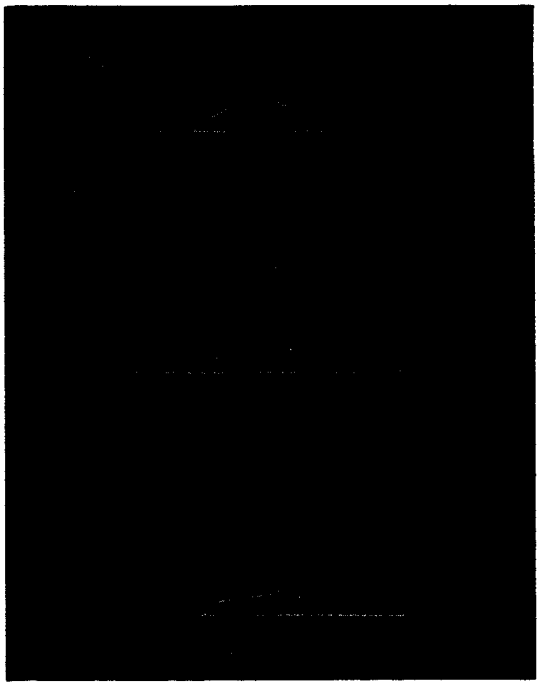

Figure 27 - Test Diode Operating Data with 3200 CPS Arc Drop

Cathode Shield:	Barium - Medium
	Molybdenum - Low
	Tungsten - Low
Ceramic:	Nickel - High
	Barium - Medium
	Manganese - Low

The nickel on the ceramic wall was probably evaporated from the cathode shield. The presence of molybdenum and tungsten on the cathode shield was the result of the necessary high operating temperature of the cathode.

It was observed that in the case of the pyrolytic impregnated graphite anode, no dusting of the graphite had occurred as it did with the porous graphite. The pyrolytic coated anode still maintained its high metallic luster. While no direct measurements were made on the gas clean-up rate in these test diodes, observations indicated that the clean-up rate was not excessive. Condensation of sputtered material around the cooler portions of the tube wall traps gas molecules permanently in the metal lattice. Besides having a low sputtering yield, any graphite sputtered to the walls would not be expected to build up a vacuum-tight layer. Gas atoms temporarily trapped at the tube wall at 800°C would have sufficient energy to migrate through the deposited layer. If necessary, a hollow anode structure could be used to minimize the clean-up rate. With this structure the density of ion impact is uniform, and the clean-up of gas by sputtering is in equilibrium with the liberation of the same mechanism from other parts of the anode surface. In either case, it is suspected that some initial gas clean-up would occur until equilibrium conditions could be set up between gas trapping and liberation.

A proposed high-temperature thyratron structure is shown schematically in Figure 28. High-temperature ceramic-to-metal seals are used along with a pyrolytic impregnated anode and grid structure. The anode would be mounted in a manner similar to the mounting of the test diode structures previously described. The cathode consists of a porous nickel substrate impregnated with a barium emission compound, supported on a vacuum-tight cylinder. The cathode heater would be bonded directly to the external side of the cathode support cylinder. The advantages with this structure are two fold: (1) the heater is external to the tube, making the tube operation independent of cathode heater voltage, and (2) it makes a rugged assembly capable of withstanding the rigors of vibration and shock. The bonded heater also increases the heat transfer efficiency over that of a radiation-type heater. This tube design also allows the anode and grid structure to be tied down to an appropriate heat sink through the mounting supports.

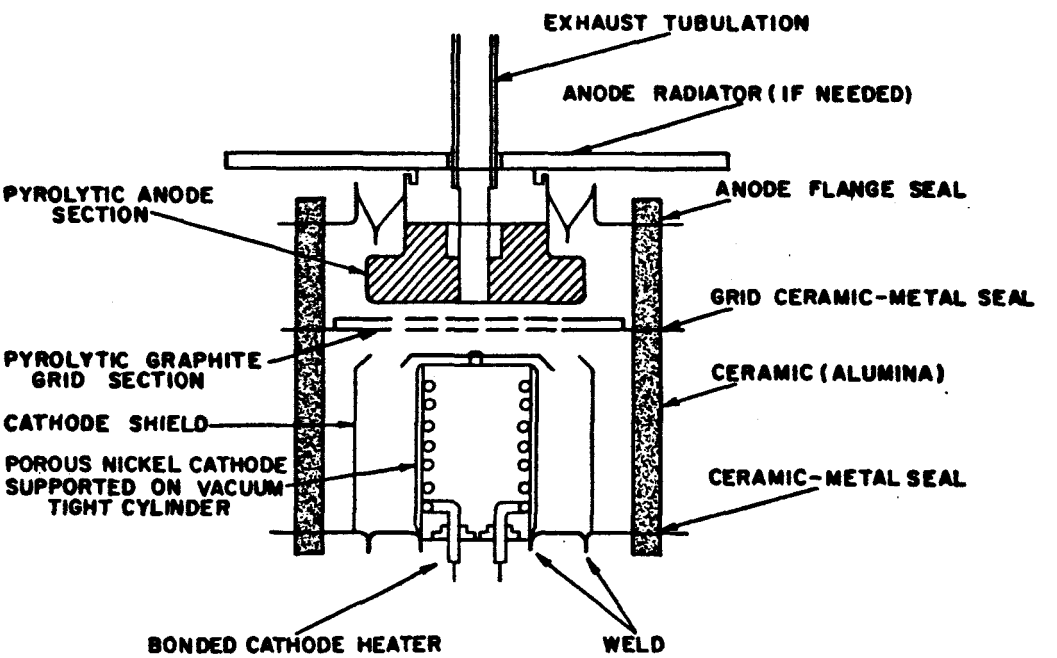

Figure 28 - Proposed High-temperature Thyratron

VOLTAGE REGULATOR AND REFERENCE TUBES

Problem Delineation

Two principal applications of the cold cathode glow discharge are in voltage regulator and voltage reference tubes. Generally these devices are operated at a temperature below 100°C. Recent[7, 8] work has extended the operating temperatures to 400°C. The volt-ampere characteristics above this temperature have not been well defined and abnormalities have been observed in the voltage stability.

Figure 29 represents a portion of the generalized volt-ampere characteristic curve for a cold cathode gas discharge. The region of interest for a voltage regulator device is the normal glow portion of the curve. In this region the tube voltage is practically independent of tube current over a fairly large range. As the circuit current is increased, the cathode current density remains relatively constant and the cathode glow extends over more of the cathode area. When the cathode area is completely covered by the glow, any further increase in current requires an increase in current density. Under this condition, higher energies are required to liberate electrons from the cathode. Tube voltage increases and the characteristics extend to the abnormal glow region (Figure 29). The particular discharge conditions are dependent on the nature of the gas, the pressure, the electrode geometry, and the cathode material. Starting voltage of a regulator tube operating in the normal glow region extends into the subnormal glow region. Sufficient voltage must be applied initially to overcome energy losses as the discharge builds up. Once the point is reached where the current can be maintained by secondary emission (α) processes at the cathode, the discharge drops to the normal glow voltage. Since the potential drop in a voltage regulator tube is primarily dependent on the gas and cathode material, various operating voltages can be obtained. The largest voltage drops generally occur with the molecular gases where drops on the order of 400 volts can be obtained. However, because of stability problems of this type of discharge at high temperatures, there is an advantage in cascading cells of lower voltage.

(7) General Electric Company, Tube Department, Feasibility Study of High Temperature Tubes, 1958-1962.

(8) J. M. Lafferty, New Voltage Regulator and Voltage Reference Tubes for Critical Environments, General Electric Technical Information Series Report RL-1803 (1957).

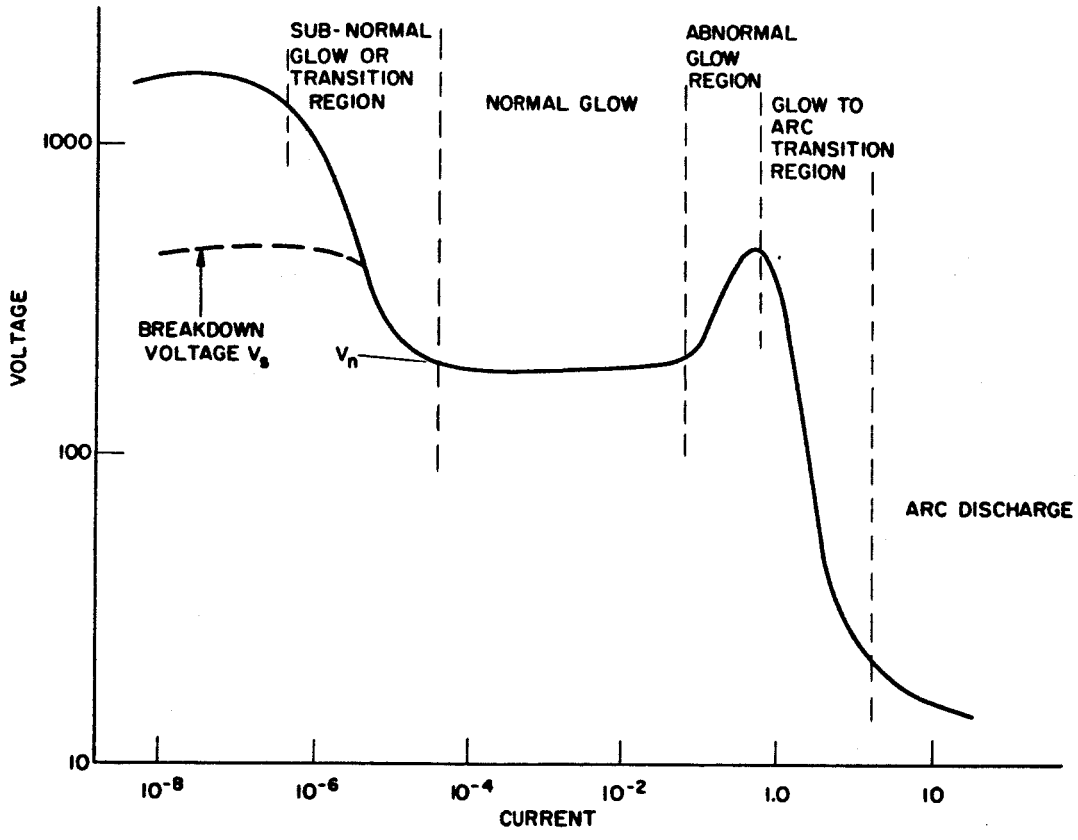

Figure 29 - Generalized Volt-Ampere Characteristics

Another application of the glow discharge is in voltage reference tubes. In this device the discharge is generally operated in the abnormal glow region of Figure 29, where the discharge covers the entire cathode surface. Operation in this mode is characterized by a high impedance, i.e., the $\Delta V/\Delta I$ is large compared to the normal glow region.

The criterion for a reference tube operating at high temperature is that the discharge voltage be stable with temperature. The glow discharge generally shows a small negative temperature coefficient over the temperature range of 25°C to 100°C. T. Jurriaanse has explained the voltage temperature variation theoretically and concludes that there is a negative temperature dependence. Benson and Burdett, and Benson and Chalmers discuss this negative temperature dependence in various rare gas mixtures. Data obtained on this program show a small negative dependence up to about 200°C to 250°C for our particular tube design. At this point, the curves indicate a positive temperature dependence. Investigations concerning the temperature dependence of operating voltage up to 800°C were made as part of this program.

Experimental Results of Voltage Regulator Tubes

Investigations were made on the volt-ampere characteristics of neon-filled regulator tubes to temperatures of 800°C. The tube structures were mounted on a vacuum and gas loading system inside a shielded radiation heater. By suitable valving, the bell-jar providing the ambient pressure could be exhausted separately, then valved off, and the tube could be exhausted, baked-out, and gas loaded. The gas loading was accomplished either by gas loading at operating temperature on the system or by gas loading at room temperature. In the latter case the loading pressure was proportional to the ratio of tube temperature at loading to the operating temperature. The loading pressure was monitored with a Wallace-Tiernan absolute pressure gage. In all cases neon was used as the working gas. Volt-ampere characteristics were obtained by automatically sweeping the current and plotting the tube voltage as a function of current on an X-Y recorder. A photograph of the exhaust and gas loading system is shown in Figure 30.

Some initial investigations were made on a tube structure designated as the Z-5301. This device consisted of a titanium matching ceramic body brazed to a planar titanium anode. The cathode was a molybdenum cup attached to a titanium header. The gas loading in this tube was such that the pressure was approximately 60 Torr at 400°C.

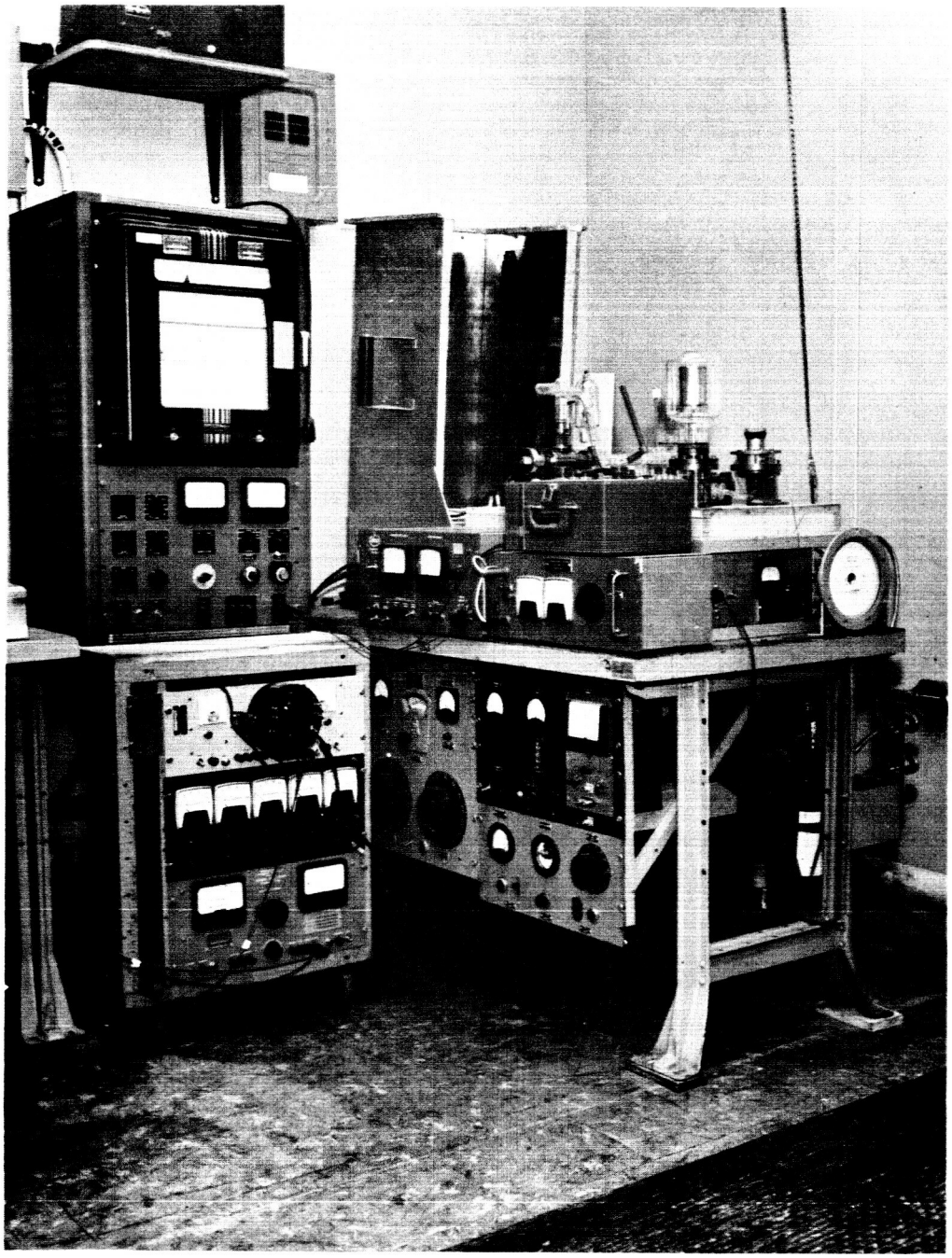

Figure 30 - Vacuum and Gas-Loading System for Voltage Regulator Test

Figures 31 and 32 show the regulating characteristics of this structure over a current range of 5 milliamperes to 50 milliamperes at 25°C and at 400°C. The characteristic at 400°C appeared to be better than that at 25°C. A small negative voltage dependence occurred in the 5 ma to 10 ma range at 25°C. Figure 33 shows data taken on the voltage variations with temperature. The current was held constant at 50 ma during this test. Up to approximately 250°C the voltage shows a negative dependence, i.e., the tube voltage decreased with increasing temperature. Above 250°C the voltage showed a positive dependence on temperature. This characteristic appeared to be typical with this type structure.

Figure 34 shows the electrode structure of a concentric anode tube on which most of the high temperature characteristics were obtained and Figure 35 shows the completed tube. The cathode is a molybdenum cup joined to a nickel support flange. The anode is a fernico tube which also serves as the exhaust and gas loading tubulation. The starting gap is provided by the spacing between the tubulation and the bottom of the molybdenum cup. Butt-type ceramic-to-metal seals of the active alloy variety were used. The seal alloy was the nickel-rich, nickel-titanium type capable of 900°C operation.

The dynamic volt-ampere characteristics for this structure while on the gas loading system are shown in Figures 36, 37, and 38 at various tube temperatures and pressures. The slopes of the curves at the higher temperature are approximately the same. It was also noticeable that hysteresis effects were less at the higher temperatures. Although this was not always the case, the broadening of the dynamic characteristic between increasing current and decreasing current generally decreased with increased gas pressure.

Figure 39 is a curve of the running voltage as a function of the ratio of tube current to ambient temperature for the concentric anode structure. The neon gas loading was adjusted so that the pressure at 800°C was approximately 60 Torr. This plot maps out the dynamic tube characteristics from 215°C to 800°C and currents from 10 ma to 75 ma for a sealed tube structure. The solid lines show the voltage change with ambient temperature at constant current, and the dashed curves show the variation in running voltage with current at constant temperature. As indicated on the curves, the regulation, i.e., $\Delta V/\Delta I$, at constant ambient temperature improved with increasing temperature. The regulation at 800°C over the range of 25 ma to 75 ma was within 3%. The temperature coefficient, $\Delta V/\Delta T_a$, was of the order of 10 mv/°C with an apparent improvement at the higher temperatures.

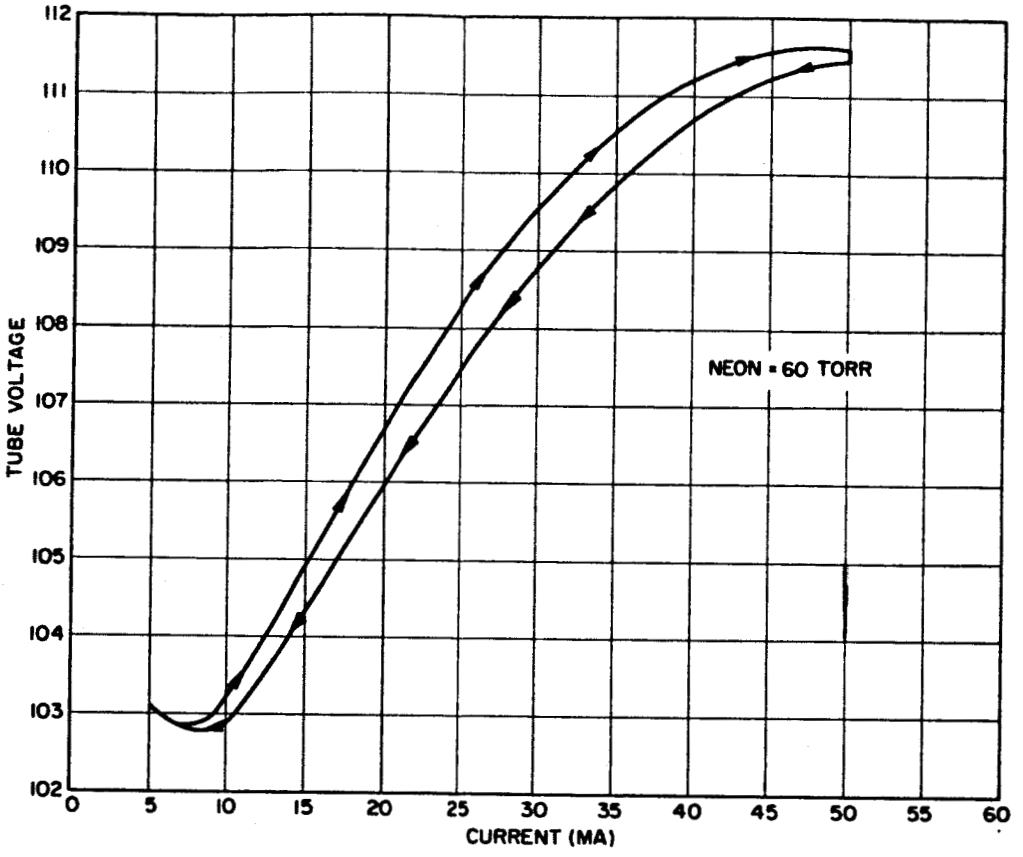

Figure 31 - Regulating Characteristics at 25°C

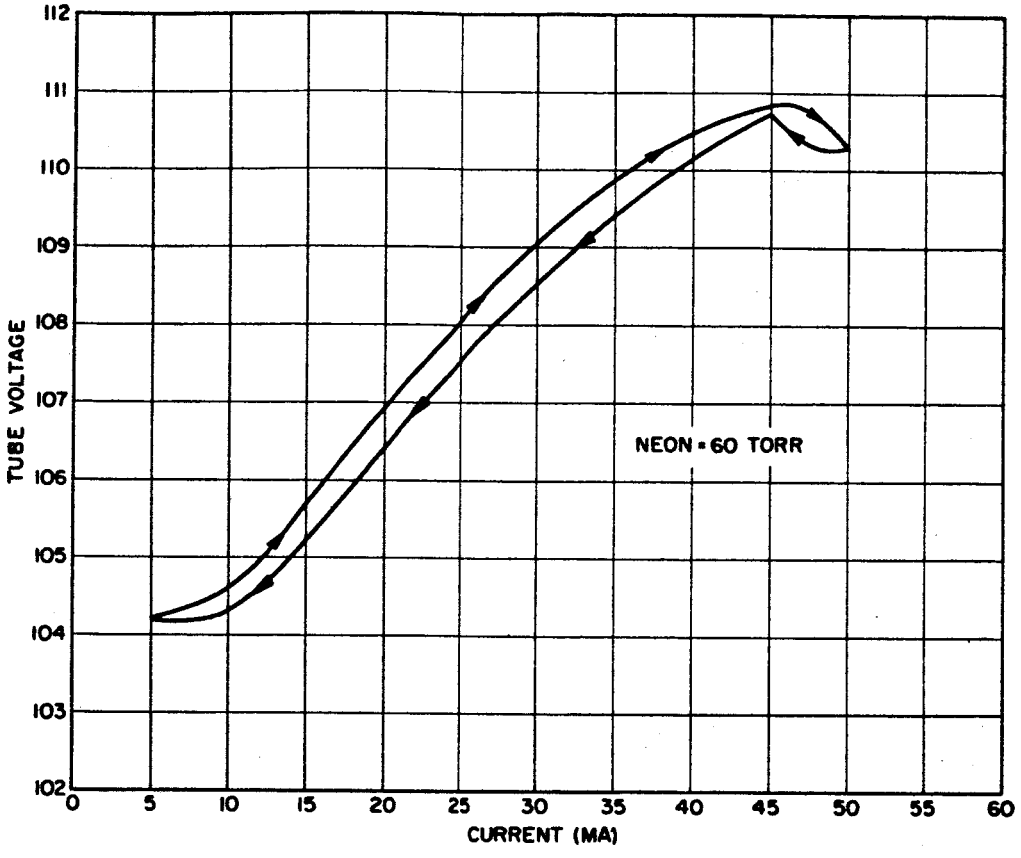

Figure 32 - Regulating Characteristics at 400°C

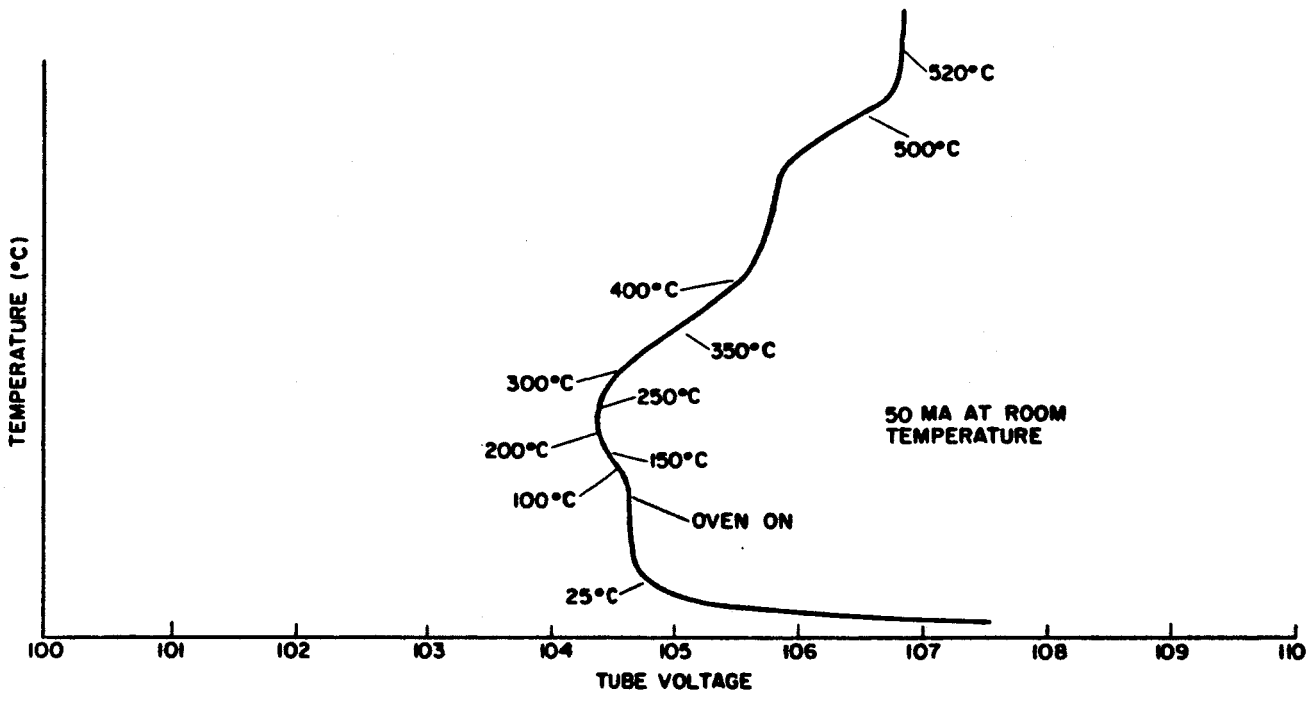

Figure 33 - Voltage Variations with Temperature

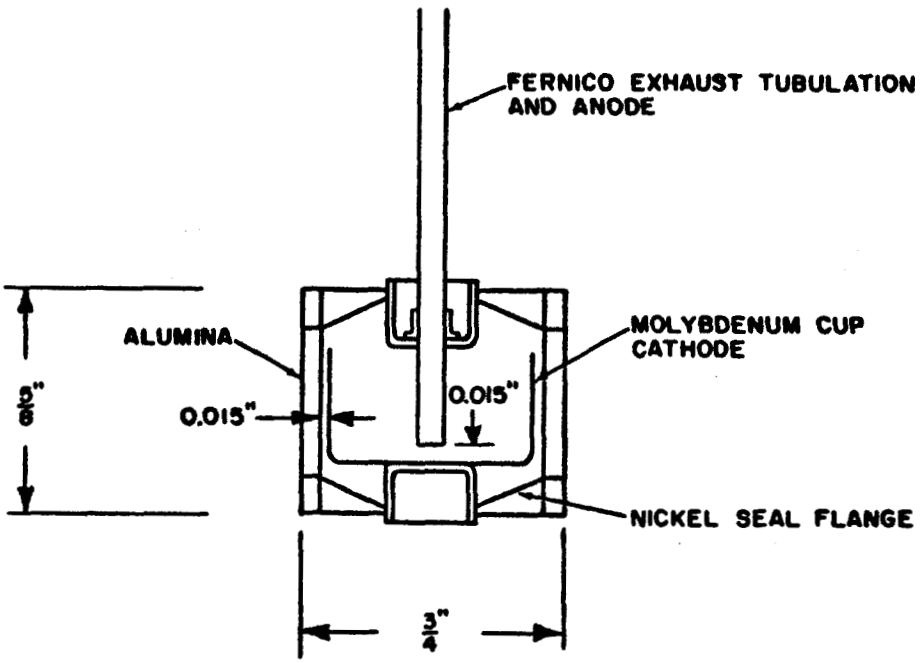

Figure 34 - Electrode Structure of a Voltage Regulator Tube Containing a Concentric Anode

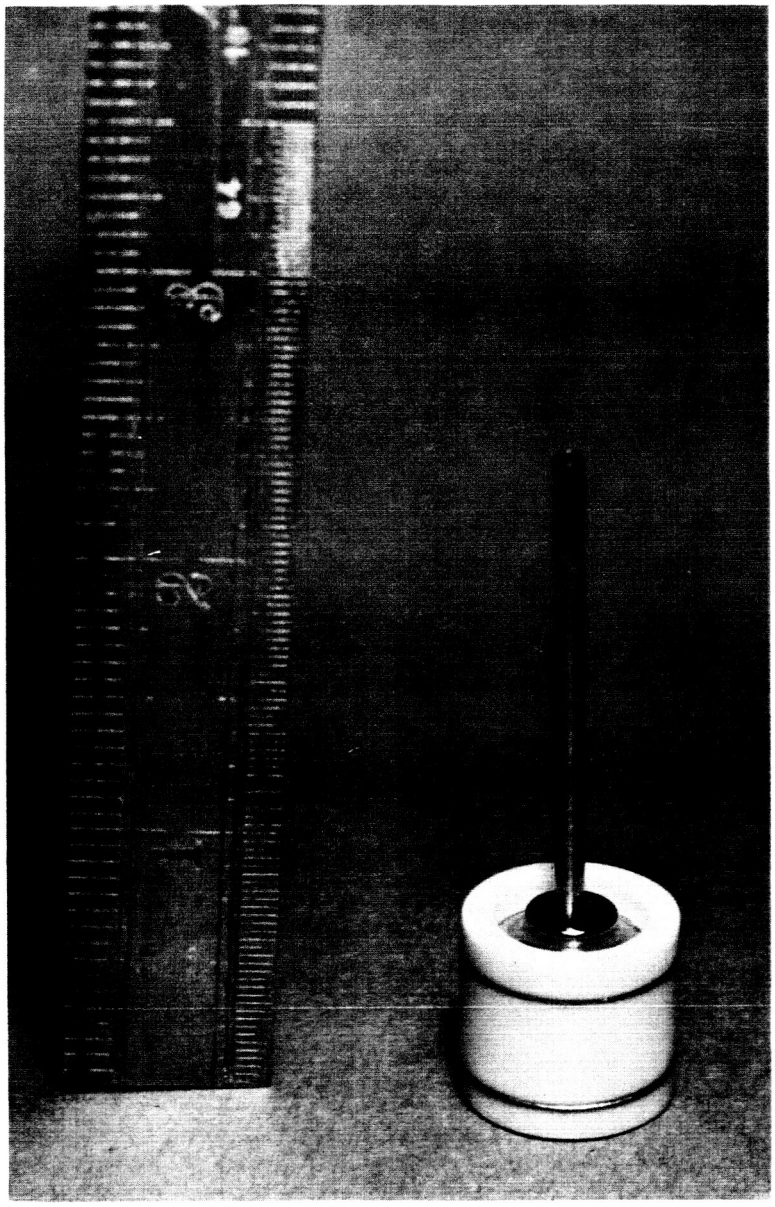

Figure 35 - A Completed Voltage Regulator Tube Containing a Concentric Anode

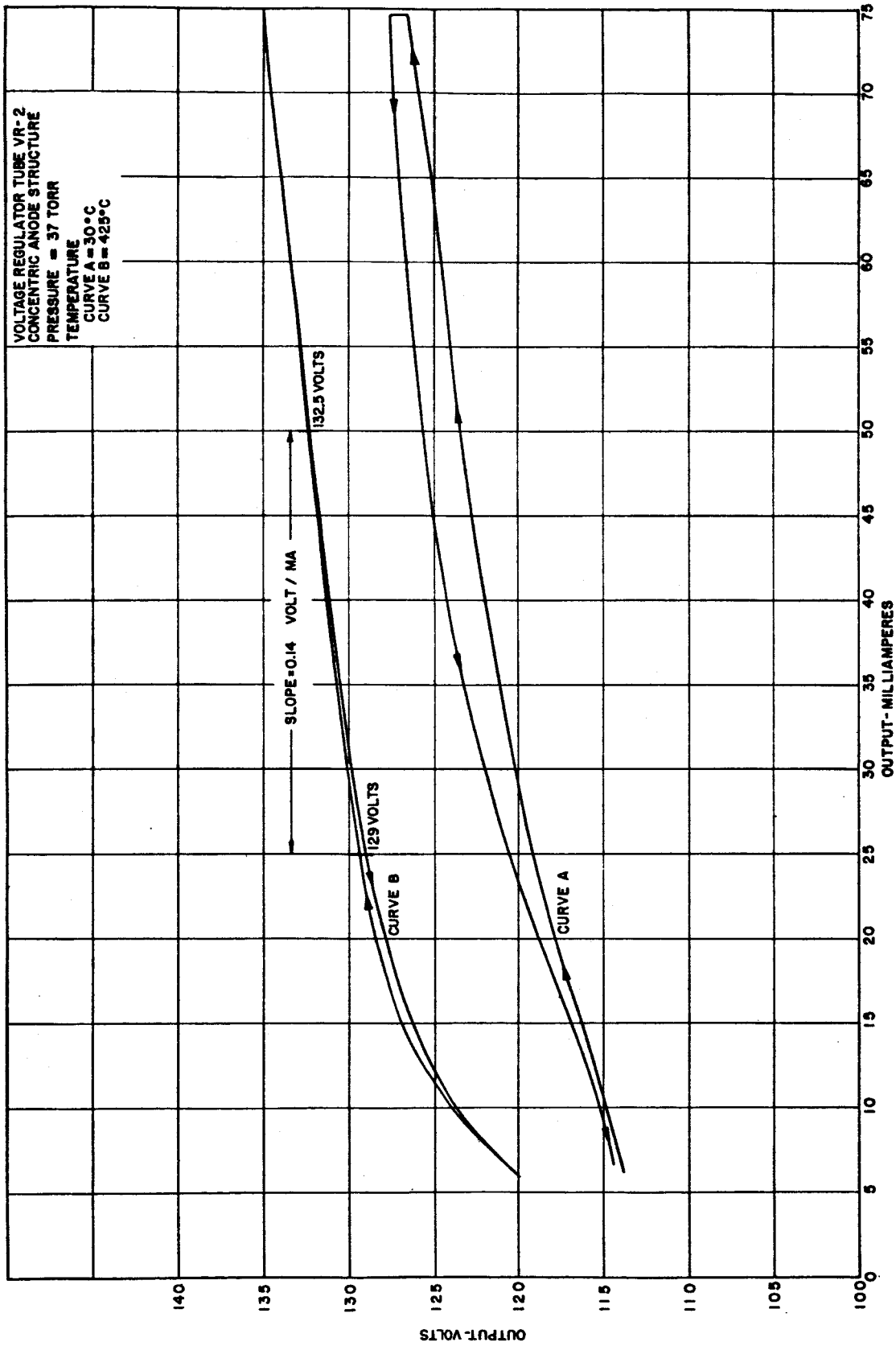

Figure 36 - Volt-Ampere Characteristics of Voltage Regulator Tube VR-2 Containing a Concentric Anode (Pressure = 37 Torr)

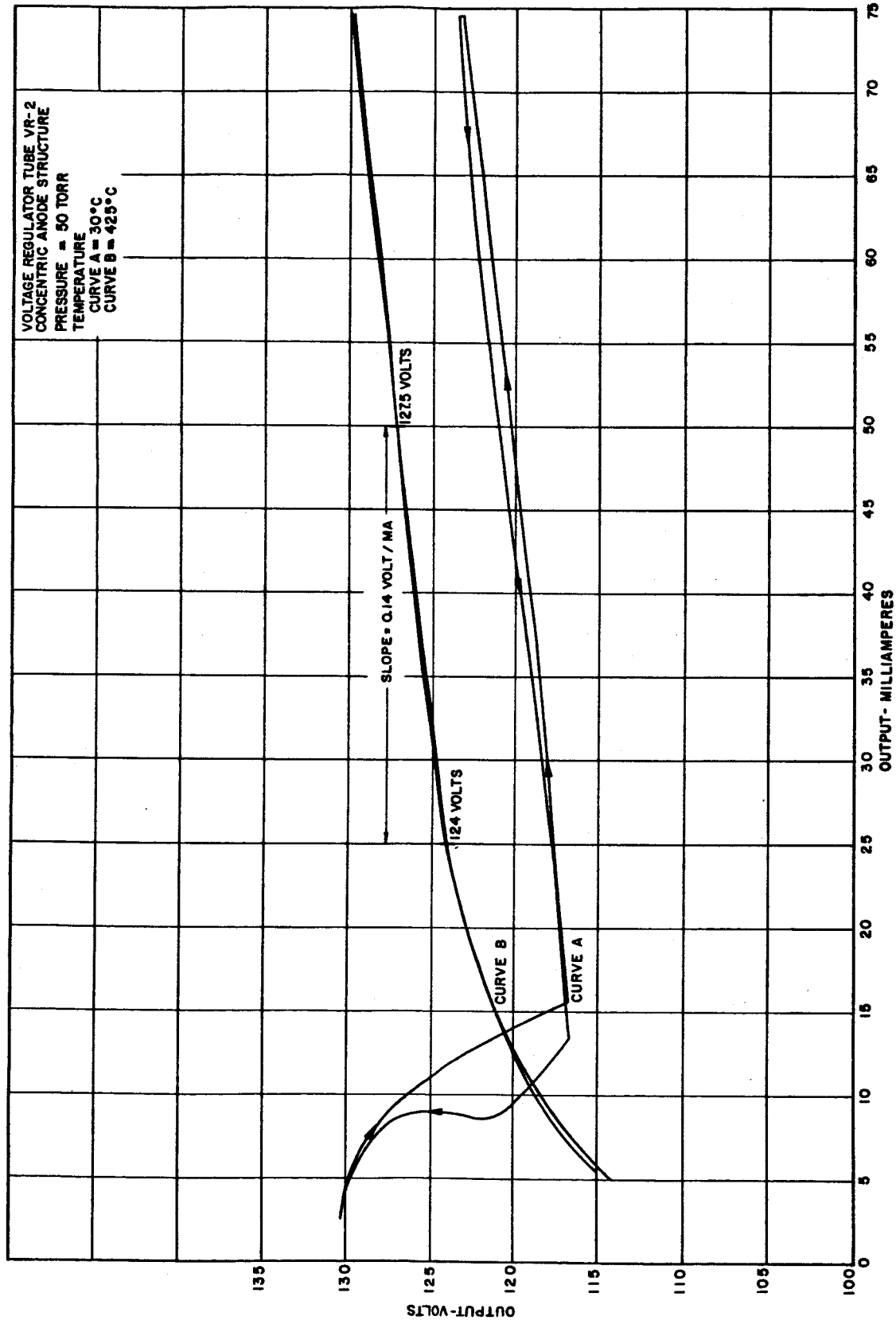

Figure 37 - Volt-Ampere Characteristics of Voltage Regulator Tube VR-2 Containing a Concentric Anode (Pressure = 50 Torr)

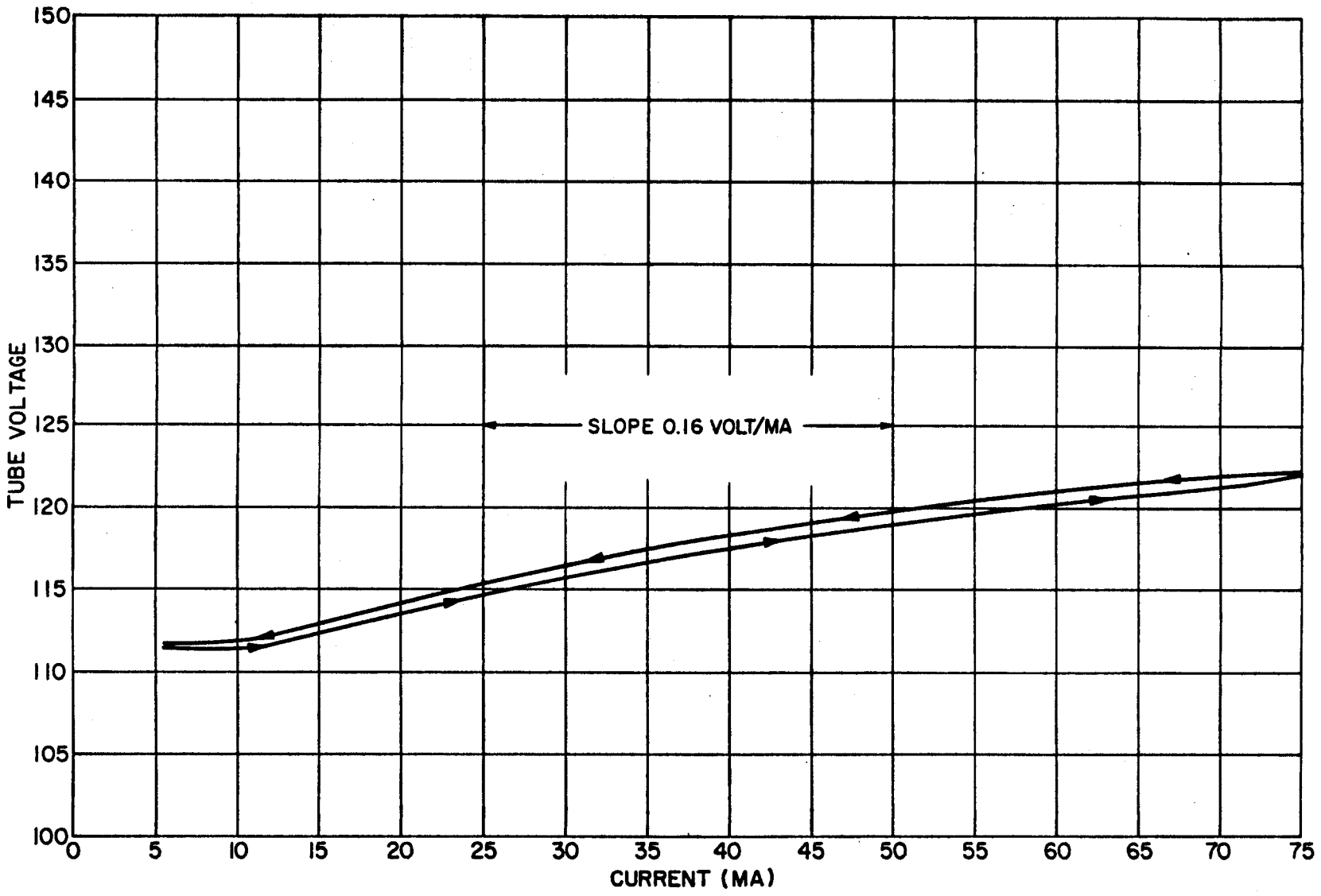

Figure 38 - Volt-Ampere Characteristics of Voltage Regulator Tube VR-2 Containing a Concentric Anode (Pressure = 60 Torr)

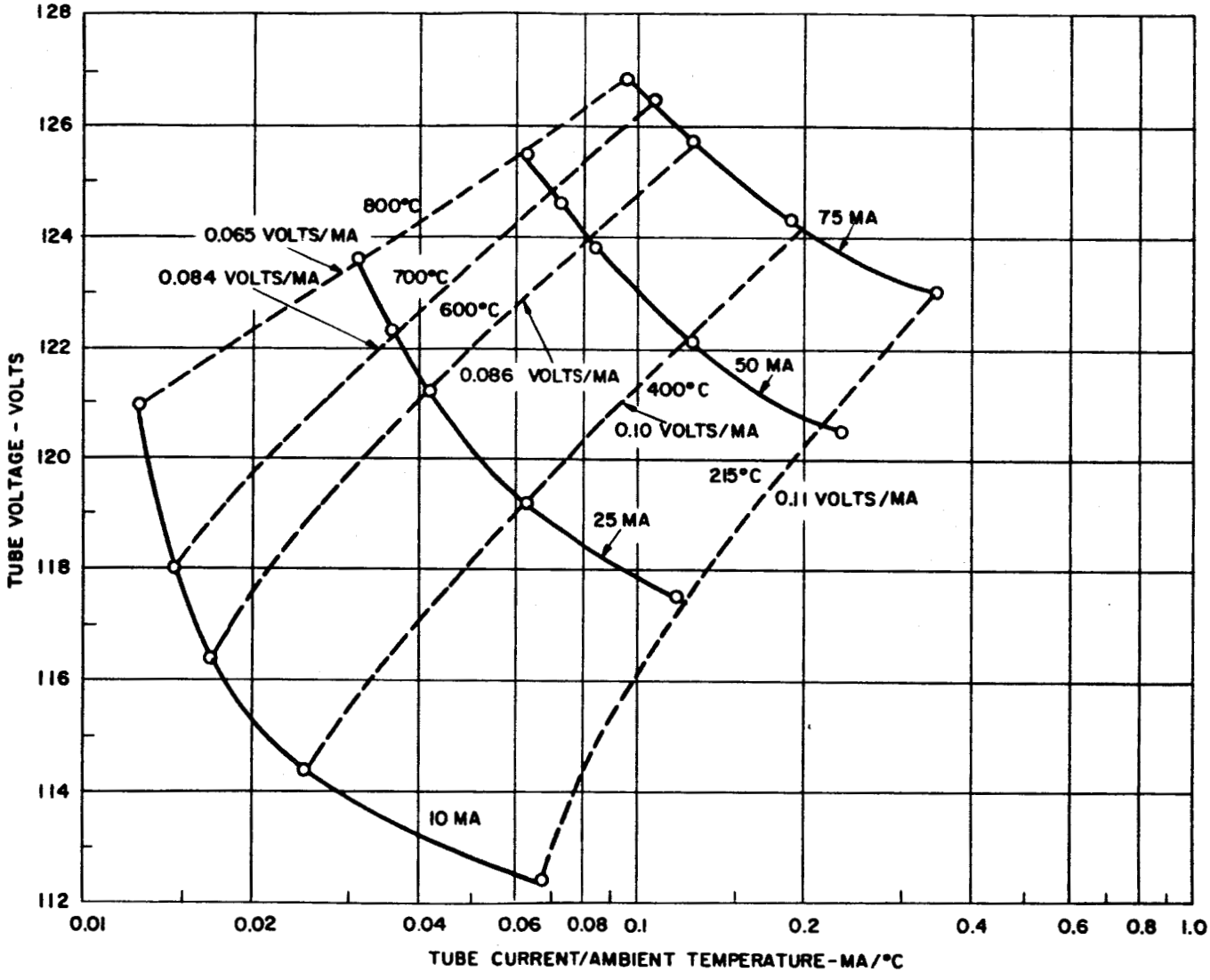

Figure 39 - Tube Voltage Versus the Ratio of Tube Current to Ambient Temperature for the Concentric Anode Voltage Regulator

Figure 40 shows a set of dynamic characteristic curves at high and low temperatures. The data for the solid curves were taken while the VR tube was on the gas loading system so that the neon could expand into the cooler section of the system. The dotted curves were taken after the tube was pinched off the gas loading system. Although the tube running voltage changed by some 2 to 5 volts, the general shape of the curves remained about the same. This presentation of the data also indicates an improvement of the regulation at the higher temperatures. This result may be explained by the fact that small changes in gas temperature due to variations in tube current do not appreciably affect the gas concentration or density distribution in the cathode region of the tube; i. e., $\Delta T_g / T_g \rightarrow 0$ at high tube temperatures.

The effects of step changes in current were observed for neon pressures of 45 and 80 Torr at a stable temperature of 800°C. Figures 41 and 42 show the stabilization times in tube voltage after 10 ma step changes in current. After each change in current the voltage was allowed to stabilize before the next change was made. The stabilization times are notably less at the higher gas pressure. At the higher pressures, the gas and tube temperatures can equilibrate more rapidly because of more efficient heat transfer. The maximum voltage transitions observed were on the order of 0.5 volt, and the equilibrium times were from 2.5 to 10 minutes.

Although no extended operational tests were required as a part of this program, one tube was run for 500 hours at 800°C in vacuum. The gas loading was neon at 60 Torr. During the last 50 to 100 hours the tube drop began to gradually increase. On examination it was found that the fernico pinch-off on the exhaust tubulation had developed a leak.

Discussion

The results of the work on this contract show the feasibility of operating voltage regulator tubes at temperatures up to 800°C. Although neon was the only gas used during these investigations with molybdenum cathodes, other combinations of gas and cathode materials can be used to adjust the starting and running voltage for a given application. However, the specific operating characteristics for different gas and cathode combinations will also have to be examined.

The results of the work effort at this time show that voltage regulator and reference tubes can be made to operate at device temperatures up to 800°C in vacuum, and voltage regulation within 3% can be achieved for relatively large variations in current. Voltage regulation of the order of

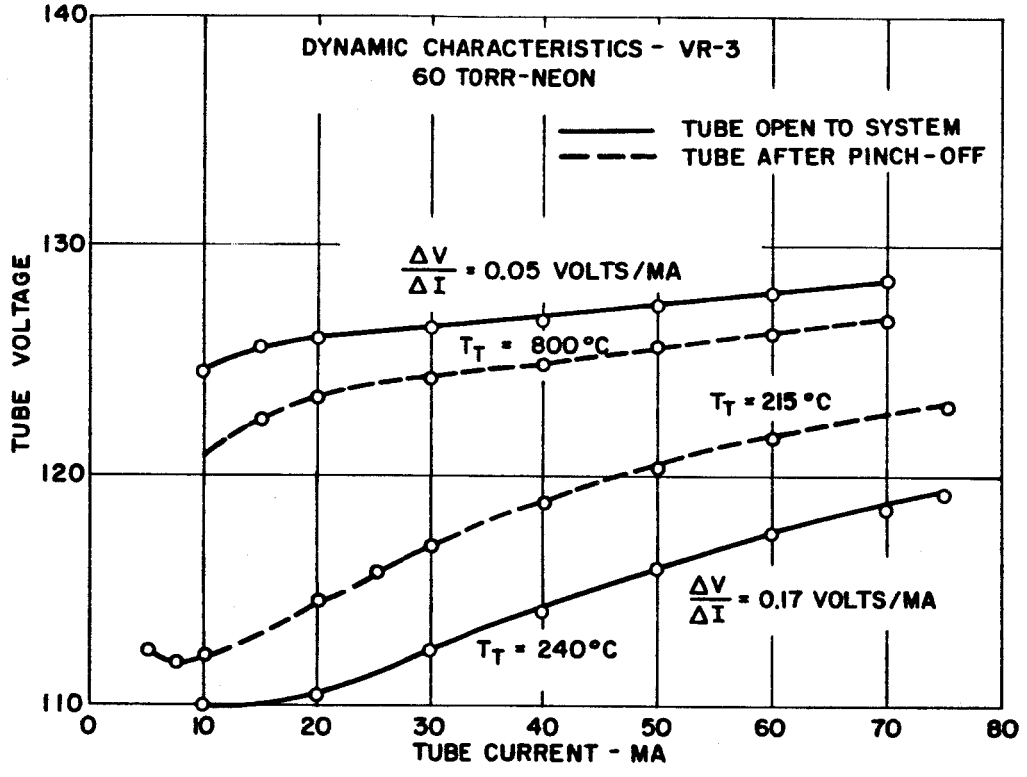

Figure 40 - Dynamic Characteristics of VR-3 at High and Low Temperatures

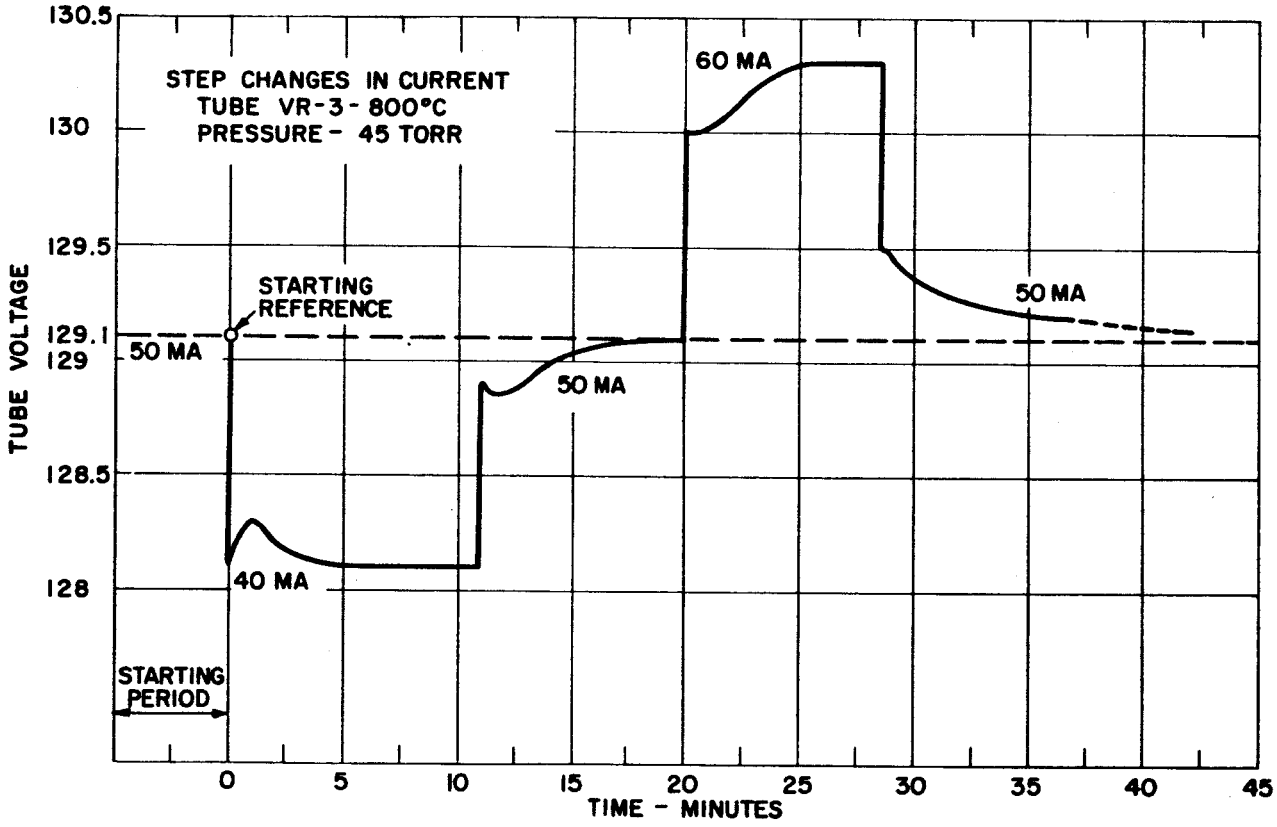

Figure 41 - Step Changes in Tube Current at Constant Ambient Temperature (Pressure = 45 Torr)

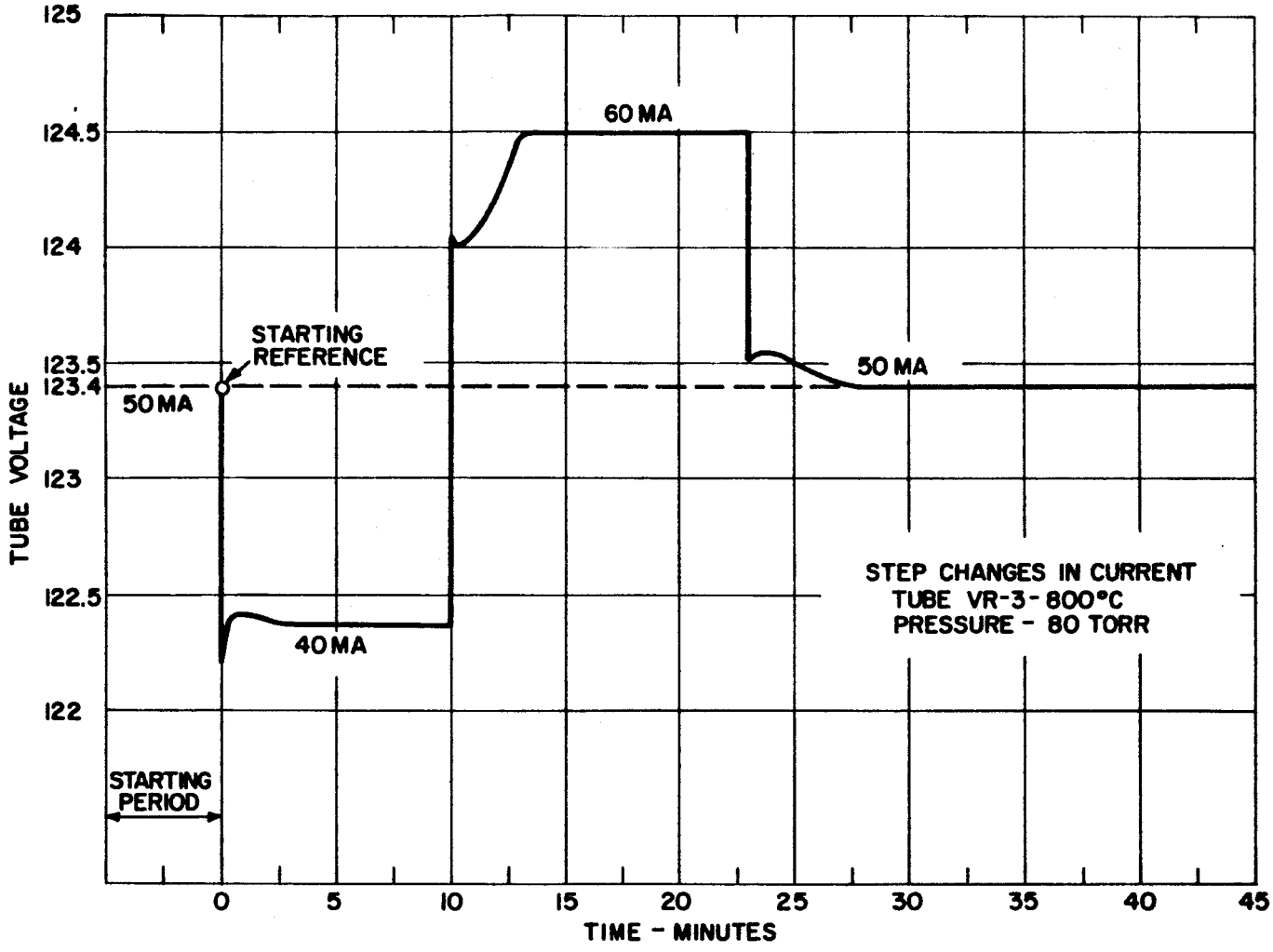

Figure 42 - Step Changes in Tube Current at Constant Ambient Temperature (Pressure = 80 Torr)

1% can be obtained at 800°C if the tube current variations are limited to approximately 10 milliamperes.

The data obtained on the concentric anode structure indicates that the regulation improved with increasing tube temperature over the entire current range. This may be explained by variations in the gas density in the cathode region due to the power dissipated in the discharge. If the running voltage depends on the gas density in the cathode fall region, then changes in tube current will produce changes in the cathode temperature, which in turn cause the local gas temperature to either increase or decrease. At the higher tube temperatures the relative change in the gas temperature may be small, resulting in only minor variations in gas density in the cathode region compared to that encountered at the lower tube temperatures. This would imply that the temperature characteristics may vary, depending on the cooling capability of the tube in the application environment.

The results of the data obtained on step changes in current indicate that the voltage drift can be relatively long before a new equilibrium is established, even though the voltage variations were within 0.5 volt. The asymptotical approach to the equilibrium value is probably due to the changes in gas density in the cathode region as the cathode temperature varied with increasing and decreasing power input.

The end of life of a glow discharge tube can occur in several different ways, such as seal failure, loss of gas filling due to vapor and ion pumping, and loss of insulation resistance between electrodes through depositing of sputtered cathode material on the ceramic walls. Although this initial work has shown that voltage regulator and reference tubes can be operated at high temperatures, extended tests are required to determine long time characteristics and modes of failure.

ABSTRACT

DEVELOPMENT OF HIGH TEMPERATURE CERAMIC RECTIFIERS, THYRATRONS, AND VOLTAGE REGULATOR TUBES

E. A. Baum

An investigation was made of the feasibility of operating ceramic-metal gas tubes in the temperature range of 600° to 800°C. Ceramic tubes of the rectifier and voltage-regulator type were operated at a tube temperature of 800°C and, in the case of the diodes, at frequencies up to 3200 cps and at a peak inverse voltage of 800 volts. The peak currents were limited in the test diodes to 6 amps.

An environmental test station was set up to evaluate ceramic seals in vacuum at temperatures up to 850°C. A total of over 2500 hours was accumulated on nickel-rich, titanium active alloy seals and metallized, gold-copper, nickel-gold, and palladium-cobalt brazed seals.

Investigations were made on possible anode materials to determine the emission characteristics due to evaporants from barium tungstate cathode. Data was obtained on the emission characteristics as a function of temperature, while continually evaporating barium to the anode surface. The results indicate that pyrolytic impregnated graphite would give minimum back emission or grid emission under actual tube conditions.

Voltage regulator tubes were operated up to 800°C in vacuum. The gas loading was neon. Dynamic volt-ampere characteristics taken over the range of 240°C to 800°C showed less voltage variation with current at 800°C than at the lower temperature. At 800°C a 2 to 3 percent change in voltage was observed over the 25 to 75 milliampere current range. The effects of step changes in current on tube voltage were also observed for neon pressures of 45 to 80 Torr at 800°C.

APPENDIX A
BIBLIOGRAPHY

Books

1. Cobine, J. D., Gaseous Conductors (Dover Publications, Inc, New York, 1958).

2. Dushman, Saul, Scientific Foundation of Vacuum Technique (John Wiley & Sons, Inc., New York, 1962), 2nd ed., J. M. Lafferty, editor.

3. von Engel, A., Ionized Gases (Oxford University Press, New York, 1955).

Contract Reports

1. General Electric Company, Power Tube Department, Feasibility Study of High Temperature Tubes, 1958-1962. Subcontract from North American Aviation under Air Force Contract No. AF33(600)-35489, "High Temperature Generator Control System."

2. General Electric Company, Power Tube Department, Investigation of Various Activator Refractory Substrate Combinations, Final Report (AFCRL-63-69), Mar. 1963. Air Force Contract No. AF19(628)-279.

3. General Electric Company, Power Tube Department, Vapor Filled Thermionic Converter Materials and Joining Problems; Plasma Research Pertinent to Thermionic Converter Operation, 15 Nov. 1961-15 Dec. 1962, Final Report. Bureau of Ships Contract No. NObs-86220.

Periodicals

1. Baker, J. A., The Use of Thermionics in the Study of Adsorption of Vapor and Gases, Trans. Faraday Soc., 28, 148 (1932).

2. Benson, F. A., and Burdett, G. P., Comparison of Argon, Krypton and Xenon as Admixtures in Neon Glow-Discharge Reference Tubes, Proc. Inst. Elec. Engrs. (London), 108, Part B, 41 (1961).

3. Benson, F. A., and Chalmers, P. M., Characteristics of Glow-Discharge Reference Tubes with Various Cathode Geometries and Surface Finishes, Proc. Inst. Elec. Engrs. (London), 109, Part B, 290 (1962).

4. Benson, F. A., and Chalmers, P. M., Effects of Argon Content on the Characteristics of Neon-Argon Glow-Discharge Reference Tubes, Inst. Elec. Engrs. (London), Monograph No. 321R (Dec. 1958).

5. Brodie, I., Jenkins, R. O., and Trodden, W. G., Evaporation of Barium from Cathodes Impregnated with Barium-Calcium-Aluminate, Jour. of Elec. and Controls, 6, 149 (1959).

6. Carmichael, J. H., and Trendelenburg, E. A., Ion Induced Re-emission of Noble Gases from a Nickel Surface, J. Appl. Phys., 29, No. 11, 1570 (1958).

7. Champion, J. A., The Grid Emitting Properties of Titanium, Brit. J. Appl. Phys., 9, No. 12 (Dec. 1958).

8. Champion, J. A., The Suppression of Screen Grid Emission by Carbon, Brit. J. Appl. Phys., 7, 395 (1956).

9. Esperson, G. A., and Rodgers, J. W., Studies on Grid Emission, IRE Transactions on Electron Devices, ED-3, No. 2 (April 1956).

10. Florio, J. V., Retarding Field Technique for Measuring Sublimation from Dispenser and Oxide Cathodes, J. Appl. Phys., 34, 200 (Jan. 1963).

11. Forman, R., Electrical Conduction and Breakdown in High-Pressure (0.25-300 mm) Rare Gases, J. Appl. Phys., 32, 1651 (1961).

12. Forman, R., Theory of Space Charge-Limited Emission in High Pressure Gas Diodes, J. Appl. Phys., 34, No. 9, 2578 (1963).

13. Forman, R., and Ghormley, J. A., Space-Charge Neutralization and Negative Resistance in Thermionic Diodes Containing Radioactive Krypton, J. Appl. Phys., 33, No. 10, 3057 (1962).

14. General Mills, Sputtering Yield Data in the 100-600 ev Energy Range, Report No. 2309 (July 15, 1962).

15. Henschke, E. B., and Derby, S. E., Threshold Energies for Cathode Sputtering, J. Appl. Phys., 34, No. 8, 2458 (1963).

16. Herring, C., and Nichols, M. H., Thermionic Emission, Revs. Modern Phys., 21, No. 2 (1949).

17. Johnson, E. O., and Walter, L., Studies of Thyratron Behavior, Part II. A Study of the Effect of Grid Potential Variations During the After Glow Upon the Recovery Time of Thyratrons, RCA Rev., 11, 178 (June 1950).

18. Jurriaanse, T., The Influence of Gas Density and Temperature on the Normal Cathode Fall of a Gas Discharge in Rare Gases, Phillips Research Report, 1, 407 (1949).

19. Jurriaanse, J., Penning, F. M., and Moubis, J. H. A., The Normal Cathode Fall for Molybdenum and Zirconium in the Rare Gases, Phillips Research Report, 1, 225 (1946).

20. Klein, C. A., Electrical Properties of Pyrolytic Graphites, Revs. Modern Phys., 34, No. 1, 56 (1962).

21. Klein, C. A., Pyrolytic Graphites, J. Appl. Phys., 33, No. 11, 3338 (1962).

22. Kok. J. A., Experiments with Gas-Filled Triodes, Appl. Sci. Research Section B, 5, 445 (1956).

23. Kok. J. A., Theory and Probe Measurements of Gabor's Gas-Filled Triode, Appl. Sci. Research, Section B, 6, 207 (1957).

24. Laegreid, N., and Wehner, G. K., Sputtering Yields of Metals for Ar^+ and Ne^+ Ions with Energies from 50 to 600 ev, J. Appl. Phys., 33, 1842 (1962).

25. Lafferty, J. M., New Voltage Regulator and Voltage Reference Tubes for Critical Environments, General Electric Technical Information Series Report RL-1803 (1957).

26. Langmuir, I., and Taylor, J. B., The Evaporation of Atoms, Ions, and Electrons from Cesium Films on Tungsten, Phys. Rev., 44, 423 (1933).

27. Levi, R., Improved "Impregnated Cathode", Jour. of Appl. Phys., 26, 639 (1955).

28. Morgulis, N. D., Physical Properties and Elements of Calculation of Porous Barium-Tungsten Cathode (L-Cathodes), Radio Eng. and Electronics, 2, No. 12, 1 (1957).

29. Morgulis, N. D., and Marchuk, A Study of the Cesium-Arc Rectifiers, J. Phys. (U. S. S. R.), 3, 95 (1958).

30. Norton, F. J., Gas Permeation through the Vacuum Envelope, Trans. 8th Vacuum Symposium, No. 2 International Congress (1961).

31. Norton, F. J., Helium Diffusion Through Glass, J. Am. Cer. Soc., 36, No. 3, 90 (1953).

32. Ptushinski, Y. G., Influence of Ion Bombardment on the Electron Emission of Porous Metal-Film Cathodes, Radio Eng. and Electronics, 2, No. 2, 46 (1957).

33. Rosenberg, D., and Wehner, G. K., Sputtering Yields for Low Energy He^+-, KR^+-, and Xe^+- Ion Bombardment, J. Appl. Phys., 33, 1842 (1962).

34. Scheer, M. D. and Fine, J., Entropies, Heats of Sublimation, and Dissociation Energies of the Cesium Halides, J. Chem. Phys., 36, No. 6, 1647 (1962).

35. Ward, A. L., Calculations of Cathode-Fall Characteristics, J. Appl. Phys., 33, No. 9, 2789 (1962).

36. Wehner, G. K., Low-Energy Sputtering Yields in Hg, Phys. Rev., 112, 1120 (1958).

37. Wehner, G. F., Sputtering Yields for Normally Incident Hg^+-ion Bombardment at Low Ion Energy, Phys. Rev., 108, 35 (1957).

38. Walter, L., and Johnson, E. O., Studies of Thyratron Behavior Part I. Effect of Grid Resistance on the Recovery Time of Thyratrons, RCA Rev., 11, 165 (June 1950).

Contract NAS3-2548

DISTRIBUTION LIST

National Aeronautics & Space Administration
Scientific & Technical Information Facility
Box 5700
Bethesda 14, Maryland
Attn: NASA Representative (2 copies plus 1 reproducible)

National Aeronautics & Space Administration
Lewis Research Center
21000 Brookpark Road
Cleveland, Ohio 44135
Attn: George Mandel

National Aeronautics & Space Administration
Lewis Research Center
21000 Brookpark Road
Cleveland, Ohio 44135
Attn: Library

National Aeronautics & Space Administration
Marshall Space Flight Center
Huntsville, Alabama
Attn: Russell H. Shelton

National Aeronautics & Space Administration
Marshall Space Flight Center
Huntsville, Alabama
Attn: Ernest Stuhlinger

National Aeronautics & Space Administration
1520 H Street, Northwest
Washington 25, D. C.
Attn: James J. Lynch

Naval Research Laboratory, Code 1572
Washington 25, D. C.
Attn: Mrs. Katherine H. Cass

North American Aviation, Inc.
Los Angeles 45, California
Attn: Advanced Electrical Projects

Oak Ridge National Laboratory
Oak Ridge, Tennessee
Attn: W. D. Manly

Office of Naval Research
Department of the Navy, Code 735
Washington 25, D. C.
Attn: E. E. Sullivan
For: Code 429

Pratt & Whitney Aircraft
East Hartford, Connecticut
Attn: Wm. Lueckel

U.S. Atomic Energy Commission
Technical Information Service Extension
P. O. Box 62
Oak Ridge, Tennessee (3 copies)

U.S. Naval Ordnance Laboratory
White Oak, Silver Spring, Maryland
Attn: Eva Lieberman, Librarian

Westinghouse Electric Corporation
Aerospace Electric Division
Lima, Ohio
Attn: Library

Westinghouse Electric Corporation
Astronuclear Laboratory
P.O. Box 10864
Pittsburgh 36, Pennsylvania
Attn: D. Foster

Aeronautical Systems Division
(ASRMFP-3)
Wright-Patterson Air Force Base, Ohio
Attn: Lester Schott (2 copies)

National Aeronautics & Space Administration
Lewis Research Center
21000 Brookpark Road
Cleveland, Ohio 44135
Attn: Norman Musial
Patent Counsel Office

Advanced Research Project Agency
The Pentagon, Washington 25, D. C.
Attn: John Huth

Air Force Institute of Technology
Wright-Patterson Air Force Base, Ohio
Attn: Commandant

Air Technical Intelligence Center
Wright-Patterson Air Force Base, Ohio
Attn: Commander

Air University Library
Maxwell Air Force Base, Alabama
Attn: Director

Commander, ARDC
Andrews Air Force Base
Washington 25, D. C.
Attn: RDTAPS, Capt. W. G. Alexander

U.S. Atomic Energy Commission
Germantown, Maryland
Attn: Lt. Col. G. M. Anderson

U. S. Atomic Energy Commission
Germantown, Maryland
Attn: Col. Douthet

AVCO
Wilmington, Massachusetts
Attn: Library

Chief, Bureau of Aeronautics
Washington 25, D. C.
Attn: C. L. Gerhardt, NP

Convair-Astronautics
5001 Kearny Villa Road
San Diego 11, California
Attn: Krafft A. Ehricke

General Electric Company
Missile & Space Vehicle Department
3198 Chestnut Street
Philadelphia 4, Pennsylvania
Attn: Edward Ray

Dr. Nathan W. Snyder
Kaiser Aerospace & Electronics Corp.
Room 2552
300 Lakeside Drive
Oakland, California 94604

Lockheed Missile & Space Division
Sunnyvale, California
Attn: Charles Burrell

National Aeronautics & Space Administration
Ames Research Center
Moffett Field, California
Attn: Library

National Aeronautics & Space Administration
Goddard Space Flight Center
Greenbelt, Maryland
Attn: Milton Schach

National Aeronautics & Space Administration
Jet Propulsion Laboratories
California Institute of Technology
4800 Oak Grove Drive
Pasadena, California
Attn: John Paulson (2 copies)

National Aeronautics & Space Administration
Langley Research Center
Langley Field, Virginia
Attn: Library

National Aeronautics & Space Administration
Lewis Research Center
21000 Brookpark Road
Cleveland, Ohio 44135
Attn: C. S. Corcoran
Space Power Systems Division

National Aeronautics & Space Administration
Lewis Research Center
21000 Brookpark Road
Cleveland Ohio 44135
Attn: B. Lubarsky
Space Power Systems Division

National Aeronautics & Space Administration
Lewis Research Center
21000 Brookpark Road
Cleveland, Ohio 44135
Attn: J. T. Kotnik
Electric Propulsion Office (2 copies)

USAF
Physical Electronics Branch
Wright-Patterson Air Force Base, Ohio
Attn: Mr. Cartmell (AVTT)

AiResearch Manufacturing Company
Sky Harbor Airport
402 South 35th Street
Phoenix, Arizona
Attn: Librarian (1 copy)
Mr. John Dannen (1 copy)

Pratt & Whitney Air Craft
CANEL
Middletown, Connecticut
Attn: Librarian (1 copy)
Dr. Robert Strouth (1 copy)

CANEL Project Office
U.S. Atomic Energy Commission
P.O. Box 1102
Middletown, Connecticut
Attn: Mr. Herbert Pennington

National Aeronautics & Space Administration
Lewis Research Center
21000 Brookpark Road
Cleveland, Ohio 44135
Attn: Mr. I. I. Pinkel MS 5-3 (1 copy)
Dr. L. Rosenblum MS 106-1 (1 copy)
R. L. Cummings MS 86-1 (1 copy)
H. A. Shumaker MS 86-1 (1 copy)
E. A. Koutnik MS 86-1 (3 copies)

Westinghouse Electric Corporation
Box 989
Lima, Ohio
Attn: P. Kueser

National Aeronautics & Space Administration
Lewis Research Center
21000 Brookpark Road
Cleveland, Ohio 44135
Attn: Roger F. Mather
Nuclear Power Technology Branch